Autophagy 8:12, 1741–1756; December 2012; © 2012 Landes Bioscience

ATP is released from autophagic vesicles to the extracellular space in a VAMP7-dependent manner

Claudio Marcelo Fader, Milton Osmar Aguilera and María Isabel Colombo*

Laboratorio de Biología Celular y Molecular–Instituto de Histología y Embriología (IHEM); Facultad de Ciencias Médicas; Universidad Nacional de Cuyo–CONICET; Mendoza, Argentina

Keywords: SNAREs, VAMP7, autophagy, autophagosome, LC3, focal adhesions, ATP

Autophagy is a normal degradative pathway that involves the sequestration of cytoplasmic components and organelles in a vacuole called autophagosome. SNAREs proteins are key molecules of the vesicle fusion machinery. Our results indicate that in a mammalian tumor cell line a subset of VAMP7 (V-SNARE)-positive vacuoles colocalize with LC3 at the cell periphery (focal adhesions) upon starvation. The re-distribution of VAMP7 positive structures is a microtubule-dependent event, with the participation of the motor protein KIF5 and the RAB7 effector RILP. Interestingly, most of the VAMP7-labeled vesicles were loaded with ATP. Moreover, in cells subjected to starvation, these structures fuse with the plasma membrane to release the nucleotide to the extracellular medium. Summarizing, our results show the molecular components involved in the release of ATP to extracellular space, which is recognized as an important autocrine/paracrine signal molecule that participates in the regulation of several cellular functions such as immunogenicity of cancer cell death or inflammation.

Introduction

In eukaryotic cells, macroautophagy (hereafter autophagy) is a conserved catabolic process by which some organelles, long-lived proteins and other cytoplasm molecules are degraded.[1] Autophagosomes are formed by the elongation and fusion of a flat membrane sac, called phagophore which engulfs cytoplasmic components in a double-membrane vacuole. Several compartments appear to contribute molecules (proteins and lipids) to form the autophagosome,[2] including the endoplasmic reticulum, Golgi, mitochondria and plasma membrane.[3-10] The amphisome, an hybrid organelle, is generated by interaction between autophagosomes with components of the endocytic pathway.[11,12] Finally, this structure can degrade the incorporated material by fusion with lysosomes, generating the autolysosome. Several signals can trigger autophagy in mammalian cells such as nutrient starvation, stress, or treatment with hormones.

Transport, docking, and fusion of vesicles with their proper target organelle requires conserved molecular machinery. SNARE proteins have a highly conserved domain (SNARE domain) which is responsible for the formation of the SNARE complex.[13] The current model claims that in neuronal exocytic events the interaction between v-SNARE and t-SNARE molecules is required. Numerous biochemical, structural, and genetic studies have shown that folding of this bundle would drive membranes to the fusion event.[14]

The VAMP tetanus toxin-insensitive, designated as TI-VAMP[15] or VAMP7[16] has a long N-terminal extension, called the Longin domain. Interestingly, this N-terminal extension plays an important role in both the localization and function of VAMP7. Indeed, the Longin domain produces an inhibitory effect on the SNARE complex formation. Previous publications have demonstrated the function of VAMP7 in endosomal vesicle trafficking to lysosomes.[16,17] The role of this SNARE in constitutive exocytosis and its participation in the fusion of MVBs (multivesicular bodies) with the plasma membrane to release exosomes into the extracellular medium was also demonstrated.[18,19] Furthermore, we have also demonstrated that the fusion between amphisomes with the lysosome requires VAMP7, allowing the completion of the autophagic pathway. In addition, a recent publication indicates that the homotypic fusion of ATG16L1 precursors, to form mature autophagosomes, also depends on VAMP7.[20]

In the present report we provide evidence that VAMP7 is necessary to deliver autophagosomes/amphisomes to focal adhesions upon autophagy induction by starvation. In addition we have shown that two endosomal trafficking proteins, KIF5 and RILP, are involved in the transport of the autophagic vacuoles to the cell periphery or toward the perinuclear region, respectively. Of note, these VAMP7-labeled vesicles are loaded with ATP and the starvation stimulus caused the delivery of the ATP-containing amphisomes toward the cell tips to fuse with the plasma membrane, releasing the ATP to the extracellular space.

*Correspondence to: María Isabel Colombo; Email: mcolombo@fcm.uncu.edu.ar
Submitted: 04/12/12; Revised: 08/07/12; Accepted: 08/16/12
http://dx.doi.org/10.4161/auto.21858

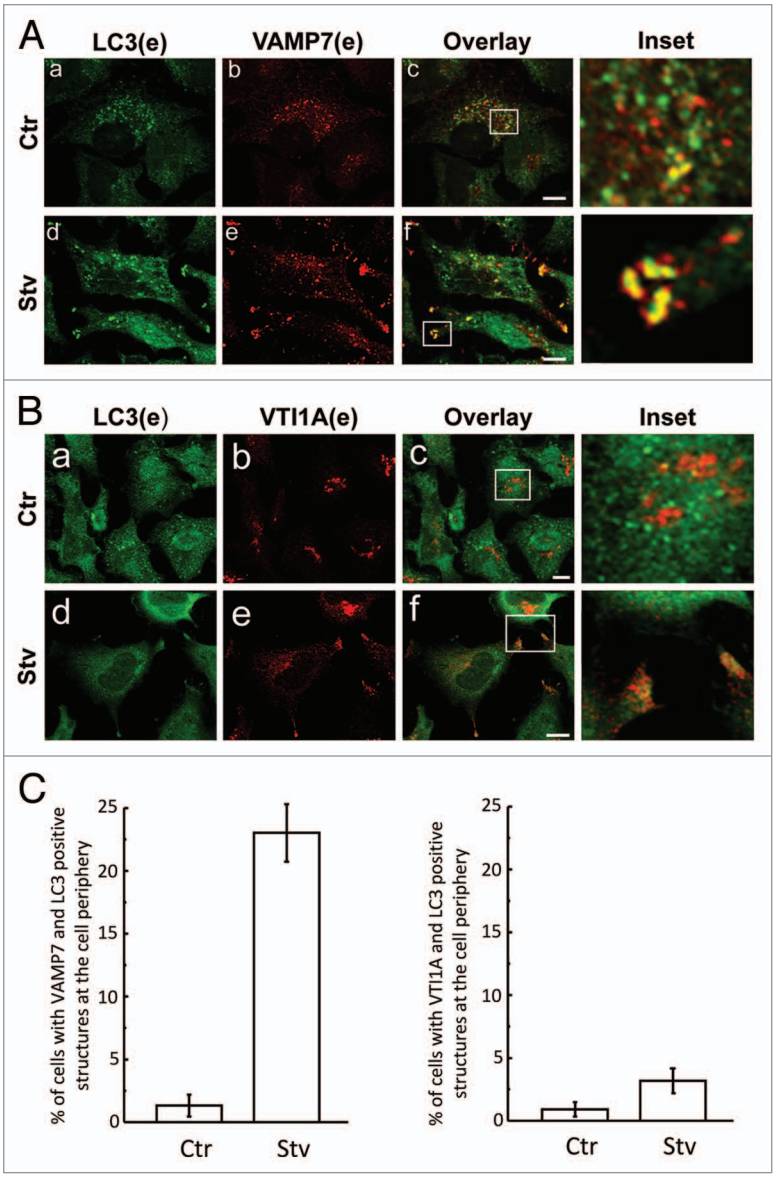

Figure 1. VAMP7- but not VTI1A-positive autophagosomes are redistributed to the cell periphery upon starvation. HeLa cells were incubated for 4 h in amino acid and serum-free media (Stv, **d–f**) or in full nutrient media (Ctr, **a–c**). Cells were fixed and LC3, VAMP7 (**A**) or VTI1A (**B**) proteins were detected by indirect immunofluorescence. Images were obtained by confocal microscopy. Scale bars: 5 μm. Mean of the Pearson's coefficient for (**A**) Ctr: 0.32, Stv: 0.69 (**B**) Ctr: 0.25, Stv: 0.39. (**C**) The percentage of cells with VAMP7 and LC3 (right panel) or VTI1A and LC3 (left panel) positive structures at the cell periphery in starvation conditions was quantified from images as the ones displayed in (**A and B**) and represent the mean ± SEM of three independent experiments. At least 100 cells were counted in each condition.

Results

Autophagy induction causes redistribution of VAMP7-labeled autophagosomes to the cell periphery. VAMP7 has been involved in multiple vesicular transport events.[17,19,21-23] In a recent publication we presented evidence that VAMP7 participates in the fusion of MVBs with the plasma membrane and also in autophagosome-lysosome fusion.[18] The protein LC3 is a representative autophagic marker[24] which localizes to autophagosomes. To investigate the possible role of VAMP7 (**Fig. 1A**) and VTI1A (**Fig. 1B**), a SNARE partner of VAMP7, in the autophagic pathway we analyzed the distribution of the endogenous proteins upon autophagy induction. VAMP7, VTI1A and LC3 were detected by indirect immunofluorescence (IF). HeLa cells were incubated in complete media (control, Ctr) or starvation media (Stv). As shown in **Figure 1A, a–c**, a fraction of LC3-positive structures were labeled with VAMP7 in full nutrient conditions, whereas no colocalization between LC3 and VTI1A was observed (**Fig. 1A, a–c**). Interestingly, upon induction of autophagy by starvation a population of VAMP7 structures, also labeled by LC3, localized at the tips of the cell (**Fig. 1A, d–f**). Similarly, a redistribution of VTI1A-vesicles also colabeled with LC3 was observed (**Fig. 1B, a–c**). The percentage of cells with VAMP7 and LC3 or VTI1A and LC3-positive structures at the cell periphery upon starvation conditions was quantified as indicated in **Figure 1C**. These results suggest that in HeLa cells starvation causes a redistribution of VAMP7-labeled autophagosomes to the cell periphery.

In order to assess whether other autophagic inducers (i.e., canonical and noncanonical)[25-27] were able to cause a similar effect, we analyzed the distribution of VAMP7 in cells treated with different compounds. HeLa cells overexpressing GFP-LC3 were incubated in starvation media (Stv) or in complete media in absence (Ctr) or presence of rapamycin (Rapa), resveratrol (Resv) or spermidine (Spd). Cells were subjected to IF to detect endogenous VAMP7. Similar to the results obtained with starvation all the others autophagic stimulators tested caused a redistribution of a fraction of VAMP7 structures, also labeled by LC3, toward the tips of the cell (**Fig. 2A**). The percentage of cells with VAMP7- and LC3-positive structures at the cell periphery was quantified as indicated in **Figure 2B** with resveratrol one of the most potent. A similar redistribution was observed in MDA MB-231 (breast cancer cell), HT-1080 (fibrosarcoma) (**Fig. S1A and S1B**) and MIO-M1 cells (Muller stem cells) (**Fig. S2A and S2B**). MDA MB-231 cells presented the higher number of VAMP7-autophagosomes at the cell periphery in autophagy- inducing conditions. As expected, the VAMP7-positive structures localized at the cell periphery upon starvation were not observed in cells incubated in the presence of wortmannin, a well known autophagy inhibitor (**Fig. S1A and S1B**). In addition, the processing of LC3 in cells incubated with the different autophagy inducers was assessed by western blot (**Fig. 2C**) and the ratio of LC3 II and tubulin was determined (**Fig. 2D**). As expected, all the autophagy inducers tested caused an increase in the LC3-II levels.

Taken together, these results suggest that in HeLa as well as in other cell types, autophagy inducers, such as starvation,

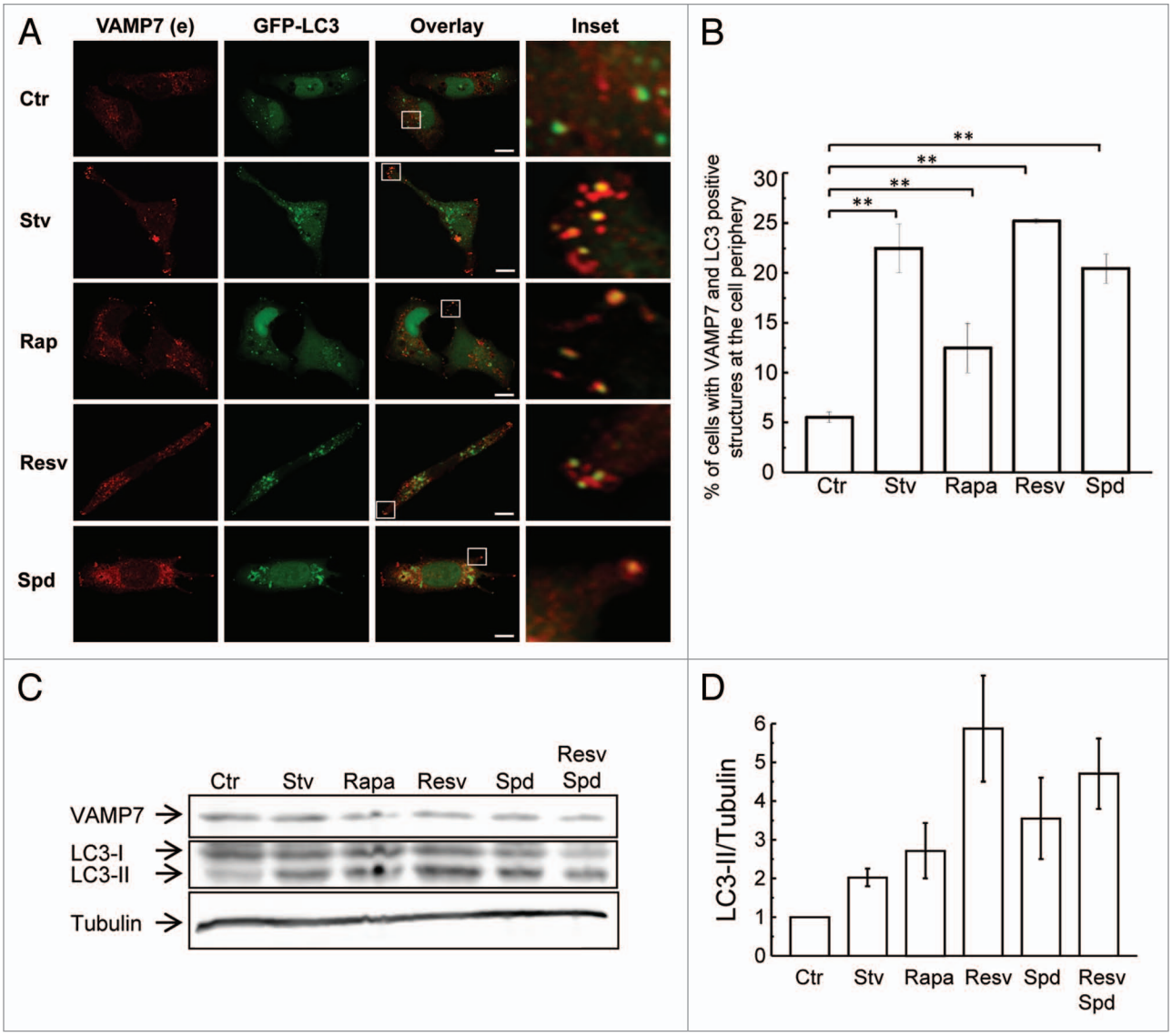

Figure 2. Autophagic inductors cause a redistribution of VAMP7-positive autophagosomes to the cell periphery. (**A**) HeLa cells overexpressing GFP-LC3 were incubated for 4 h in starvation media (Stv) or 3 h in complete media in the absence (Ctr) or presence of rapamycin (Rapa), resveratrol (Resv) or spermidine (Spd). Cells were fixed and VAMP7 was detected by indirect immunofluorescence. Images were obtained by confocal microscopy. Scale bars: 5 μm. Mean of the Pearson's coefficient are Ctr: 0.23, Stv: 0.8, Rapa: 0.76, Resv: 0.83, Spd: 0.79. (**B**) The percentage of cells with VAMP7 and LC3-positive structures at the cell periphery was quantified from images as those displayed in (**A**) and represent the mean ± SEM of two independent experiments. ** Significantly different from the control, $p < 0.005$. (**C**) HeLa cells incubated for 4 h in starvation media (Stv) or 3 h in complete media (Ctr) in the absence or presence of rapamycin (Rapa), resveratrol (Resv), spermidine (Spd) or resveratrol + spermidine (Resv + Spd) were lysed with 1% Triton X100 in PBS. Samples were subjected to SDS-PAGE and transferred onto a nitrocellulose membrane as described in Materials and Methods. The membrane was incubated with a rabbit anti-LC3, a mouse anti-VAMP7 and the corresponding HRP-labeled secondary antibodies, and subsequently developed with an enhanced chemiluminescence detection kit. (**D**) The LC3-II/tubulin ratio was measured from images as those displayed in (**C**). Images are representative of two independent experiments.

rapamycin, resveratrol or spermidine, cause a re-distribution of VAMP7-labeled autophagosomes to the cell periphery.

VAMP7-labeled structures localize in focal adhesions upon starvation. Cell-matrix interactions are involved in several physiological and pathological processes. These interactions are mainly dependent on cell surface integrins which are clustered in isolated areas of the membrane known as focal adhesions.[28] To address whether VAMP7-labeled structures distributed to focal adhesions we examined the co-localization of endogenous VAMP7 with two structural proteins PXN/paxillin and VCL/vinculin, commonly used as markers of cell matrix adhesion complexes. HeLa cells overexpressing GFP-PXN (**Fig. 3A**) and GFP-VCL (**Fig. 3B**) were incubated in complete media (control, Ctr) or in starvation media to activate autophagy (Stv). Cells were subjected to IF to detect endogenous VAMP7. Interestingly, no colocalization was observed between the focal adhesion markers and VAMP7 in control conditions (**Fig. 3B**, upper panels). In contrast, a population of VAMP7-labeled structures clearly

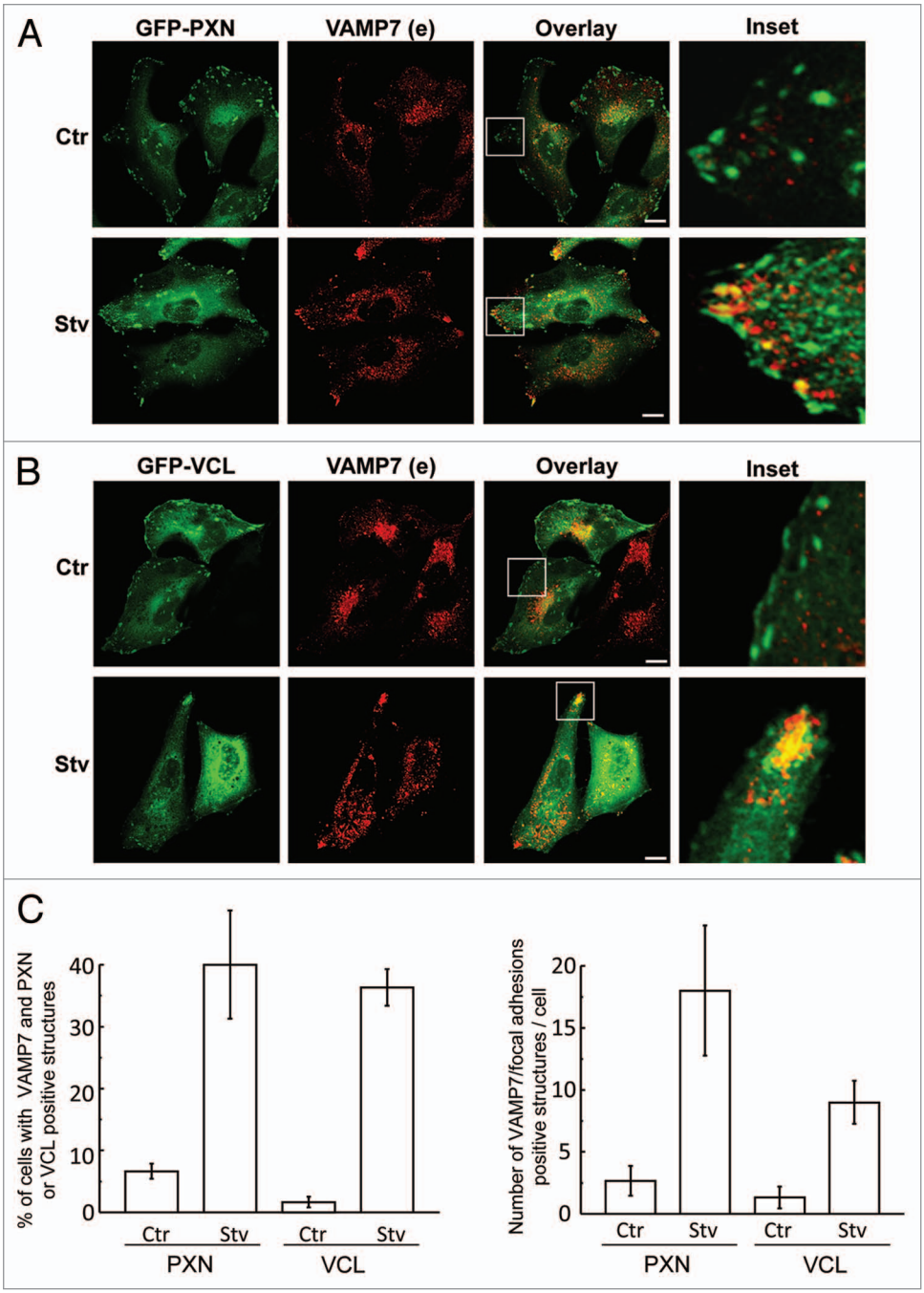

Figure 3. VAMP7-labeled vesicles are localized at the focal adhesions in starvation conditions. Transfected HeLa cells overexpressing pEGFP-PXN (**A**) or pGFP-VCL (**B**) were incubated for 4 h in amino acid and serum-free media (Stv) or in full nutrient media (Ctr). Cells were fixed and VAMP7 (red) protein was detected by indirect immunofluorescence. Images were obtained by confocal microscopy. Scale bars: 5 μm. Mean of the Pearson's coefficient for (**A**) Ctr: 0.22, Stv: 0.81 (**B**) Ctr: 0.25, Stv: 0.8. (**C**) The percentage of cells with VAMP7 and PXN or VCL positive structures (left panel) as well as the number of VAMP7/focal adhesions positive structures per cell (right panel) was determined from images as those displayed in (**A and B**) and represent the mean ± SEM of two independent experiments. At least 50 cells were counted in each condition.

colocalized with GFP-PXN (**Fig. 3A**, lower panels) or GFP-VCL (**Fig. 3B**, lower panels). The percentage of colocalization between VAMP7 and PXN or VCL (**Fig. 3C**, left panel), as well as the number of VAMP7/focal adhesion-positive structures per cell, were determined (**Fig. 3C**, right panel). These results suggest that starvation leads to an increase of VAMP7-positive structures colocalizing at focal adhesions.

The VAMP7-labeled autophagic structures localized at the cell tips have amphisome characteristics. To characterize the VAMP7 structures at the focal adhesions we analyzed the colocalization with different endosomal markers in HeLa cells incubated in starvation or in complete media. A subset of cells was incubated with the lysosomal marker LysoTracker Red and then endogenous VAMP7 was detected. As shown in **Figure 4A**, only very few VAMP7 structures, localized at focal adhesions, were labeled with LysoTracker Red (**Fig. 4A, d–f**), suggesting that these vesicles do not have lysosomal features. The percentage of cells with VAMP7 and LysoTracker positive structures at the cell periphery was determined (**Fig. 4A**, right panel). We also analyzed HeLa cells overexpressing GFP-LAMP1 (lysosomal marker) incubated in complete media or starvation media, and endogenous CTSD/cathepsin D and VAMP7 were detected by IF. As expected, in cells incubated in complete medium, a population of lysosomes close to the perinuclear region was decorated by VAMP7 (**Fig. 4B, a–d**). In contrast, in cells incubated under starvation conditions VAMP7-decorated vesicles were present at focal adhesions but no major colocalization with LAMP1 or CTSD was observed (**e–h** and **Figure 4B**, right panel).

To study the possibility that the VAMP7-labeled structures present at the focal adhesions contain early endosome markers we analyzed HeLa cells overexpressing GFP-RAB5 and endogenous CTSD and VAMP7 were detected by IF. As expected, there was no colocalization between VAMP7 or CTSD with RAB5 in control conditions (**Fig. 4C, a–d**). In cells incubated under starvation conditions RAB5-positive structures changed its distribution to a peripheral localization but no colocalization with VAMP7 or CTSD structures was observed (**Fig. 4C, e–h**). The percentage of cells with VAMP7,

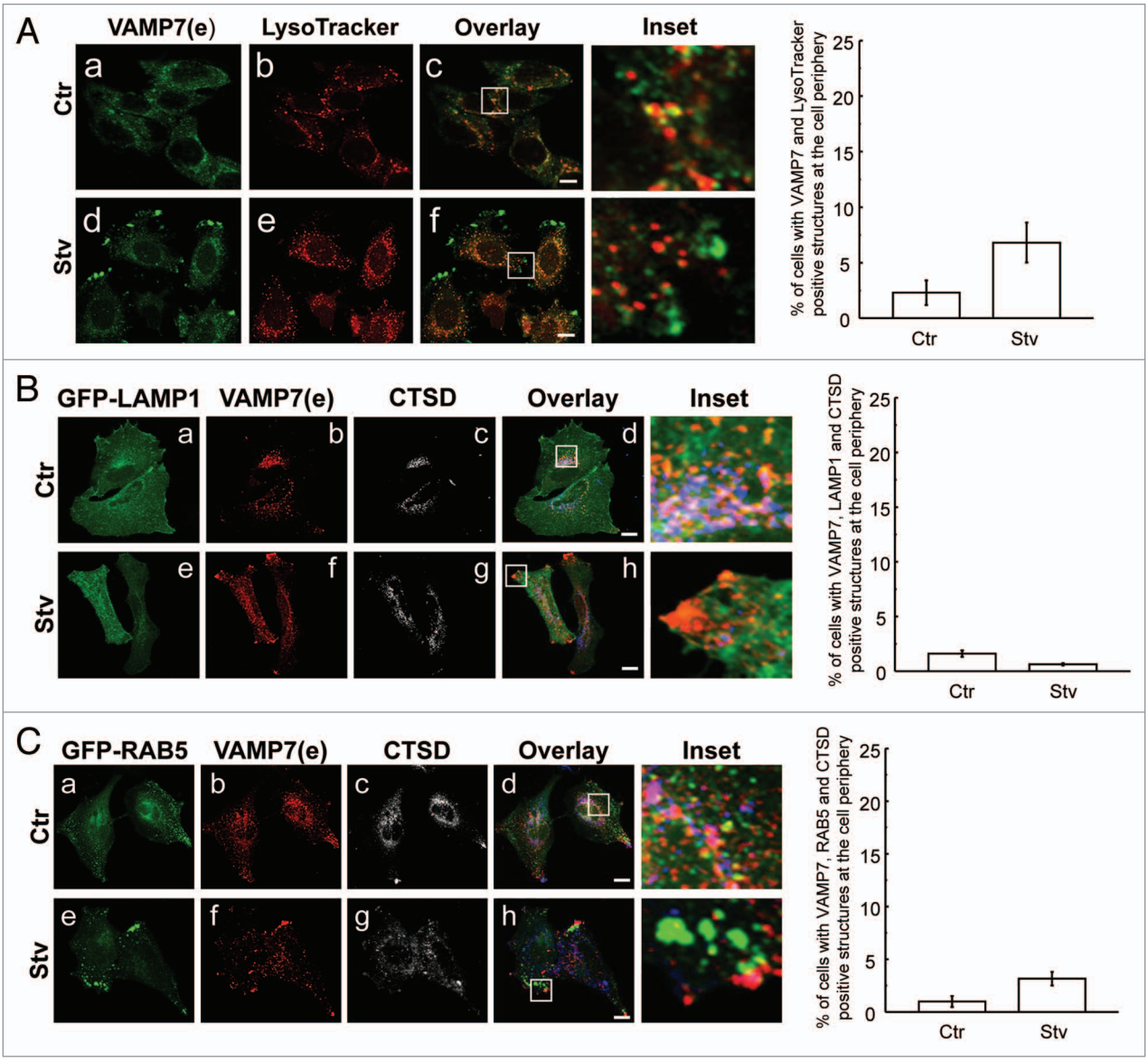

Figure 4. VAMP7 structures redistributed by starvation are only partially labeled with lysosomal markers. HeLa cells were incubated in starvation media (**d–f**) or in complete media (**a–c**). (**A**) Cells were incubated with LysoTracker Red and then endogenous VAMP7 (green) was detected by indirect immunofluorescence. Mean of the Pearson's coefficient Ctr: 0.29, Stv: 0.27. (**B**) HeLa cells overexpressing GFP-LAMP1 (lysosomal marker) were incubated in complete media or starvation media. Endogenous CTSD (blue) and VAMP7 (red) were detected by indirect immunofluorescence (IF). Mean of the Pearson's coefficient Ctr: 0.26, Stv: 0.21. (**C**) HeLa cells overexpressing GFP-RAB5 were incubated in complete media or starvation media. Endogenous CTSD (blue) and VAMP7 (red) were detected by indirect IF. Mean of Pearson's coefficient Ctr: 0.21, Stv: 0.21. Images were obtained by confocal microscopy. Scale bars: 5 μm.

RAB5 and CTSD positive structures at the cell periphery was quantified (**Fig. 4C**, right panel). In addition, cells cotransfected with GFP-RAB5 and RFP-LC3 were analyzed and as shown in **Figure S3**, both RAB5 and LC3-labeled structures changed their distribution in starvation conditions but no colocalization was observed. This result confirms that the LC3 structures present at focal adhesions (i.e., autophagosomes) are not labeled with early endosomal markers.

We next analyzed the distribution of the late endosomal marker manose-6-phosphate receptor (M6PR). Cells were incubated in the conditions mentioned above and the endogenous proteins VAMP7 and M6PR were detected. As shown in the **Figure 5A**, there was a marked increase in the colocalization between VAMP7 and M6PR near the cell edge (focal adhesions) in cells incubated under starvation conditions (**Fig. 5A, d–f** and right panel).

Since we have previously shown that RAB7 is recruited to the autophagosomal membrane and is required for autophagosome maturation[29,30] we were interested in addressing whether this RAB protein also labels the LC3/VAMP7-positive vacuoles recruited to focal adhesions. For this purpose, HeLa cells were transiently cotransfected with GFP-RAB7, incubated in complete

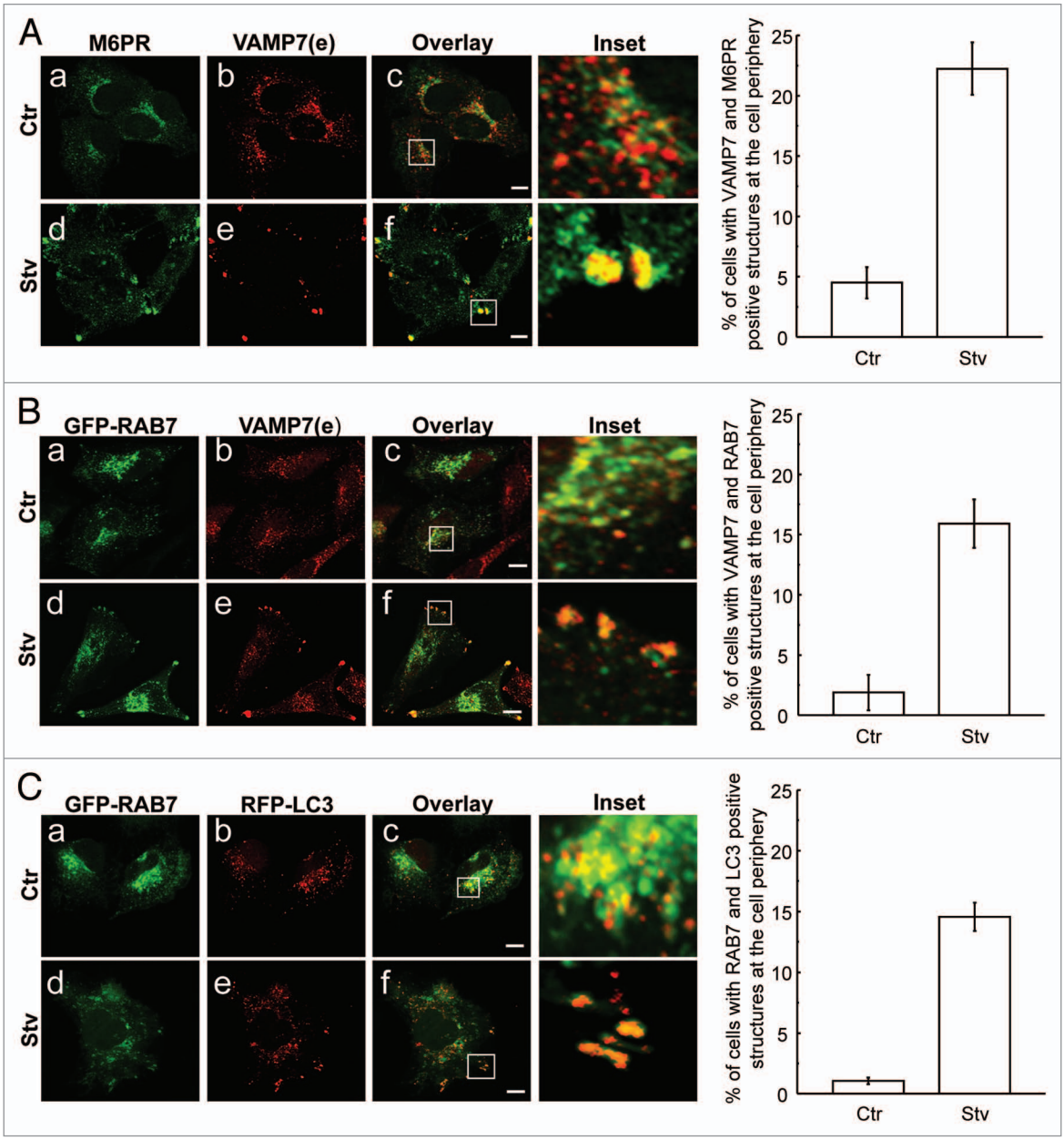

Figure 5. Late endosomal markers colocalize with VAMP7 at the cell tips upon starvation conditions. (**A**) Endogenous VAMP7 (red) and M6PR (green) were detected by indirect immunofluorescence (IF). Mean of Pearson's coefficient Ctr: 0.41, Stv: 0.82. Images were obtained by confocal microscopy. (**B**) HeLa cells overexpressing GFP-RAB7 were incubated in complete media or starvation media. Endogenous VAMP7 (red) was detected by indirect IF. Mean of Pearson's coefficient Ctr: 0.34, Stv: 0.76. Images were obtained by confocal microscopy. (**C**) Transiently cotransfected HeLa cells overexpressing GFP-RAB7 and RFP-LC3 were incubated in complete media or starvation media. Mean of Pearson's coefficient Ctr: 0.21, Stv: 0.77. Cells were mounted on coverslips and immediately analyzed by confocal microscopy. Scale bars: 5 μm.

or starvation media and then VAMP7 was detected by indirect IF. Interestingly, a high level of colocalization of RAB7 and VAMP7 at the cell periphery was observed in starvation conditions (**Fig. 5B**, see quantification in right panel), confirming the late endosomal characteristics of the VAMP7-labeled structures localized at focal adhesions. In addition, we analyzed whether these RAB7-positive structures were also labeled with LC3. Cells were transiently cotransfected with RFP-LC3 and GFP-RAB7 and autophagy was induced by starvation media. As shown in **Figure 5C**, RAB7-positive autophagosomes were localized at focal adhesions after starvation-induced autophagy. The percentage of cells with VAMP7 and LC3 positive structures at the cell periphery was determined (**Fig. 5C**, right panel). Taken together, these data suggest that autophagosomes with late characteristics (i.e., amphisomes) are recruited to focal adhesions in cell incubated in amino acid and serum free media.

VAMP7 is required for the redistribution of amphisomes toward the cell periphery. To address whether the unexpected distribution of LC3 was dependent on VAMP7, a subset of HeLa cells was cotransfected with a RFP-LC3 plasmid and a scrambled

siRNA or a siRNA against *VAMP7*. Endogenous VAMP7 was detected by indirect IF. As shown in **Figure 6A** silencing of VAMP7 caused a marked decrease of LC3-positive structures present at the cell tips but also a reduction in the total number of LC3-labeled structures, suggesting that VAMP7 is required for autophagosome formation. In order to corroborate that the knockdown of VAMP7 is affecting autophagosome biogenesis, the levels of LC3-II were analyzed by western blot. In addition we also assessed whether VTI1A was involved in the process. HeLa cells were transfected with a scrambled siRNA (Ctr) or a siRNA against *VAMP7* or *VTI1A*. The specific reduction in the amount of either VAMP7 or VTI1A is shown in **Figure 6B** (see also quantifications in **Fig. 6C and D**). Interestingly, the levels of LC3 II were only reduced in cells transfected with the *VAMP7* siRNA (**Fig. 6B and E**). These results indicate that VAMP7 but not VTI1A is required for autophagosome formation.

We next analyzed whether overexpression of the N-terminal extension of VAMP7, which hampers SNARE pairing, affects the distribution of endogenous VAMP7 close to the plasma membrane. For this purpose transiently transfected HeLa cells overexpressing the N-terminal domain of VAMP7 as a fusion protein with GFP (GFP NT-VAMP7) were generated. The cells were incubated in starvation or in complete media and subsequently subjected to IF to detect VAMP7 and CTSD. Images were taken with high and low gain in each condition to visualize either endogenous or overexpressed VAMP7, respectively. As expected, a diffuse distribution of GFP-NT-VAMP7 was observed in cells incubated either in starvation or control conditions (**Fig. S4B**). In contrast, nontransfected cells presented a typical punctate distribution of VAMP7. Interestingly, the N-terminal fragment of VAMP7 impaired the cell periphery distribution of endogenous VAMP7 under starvation conditions. The number of VAMP7 vesicles close to the cell surface upon starvation-induced autophagy was quantified (**Fig. S4C**), confirming the significant decreased percentage of these vesicles close to plasma membrane. These results suggest that starvation leads to a redistribution of VAMP7-positive structures close to the plasma membrane which is impaired by overexpression of the NT-domain of VAMP7, likely by competition of the N-terminal extension of VAMP7 with the endogenous VAMP7.

ATG5 and BECN1/Beclin 1 are required for the redistribution of the VAMP7-structures to focal adhesions upon autophagy induction. To study the possible role of some ATG proteins in the autophagy-induced transport of VAMP7-positive structures at the cell periphery, a subset of HeLa cells was cotransfected with a GFP-Vector plasmid and a pSUPER scrambled or a pSUPER BECN1^{KD}. Cells were incubated in starvation media (Stv) or in complete media in the absence (Ctr) or presence of resveratrol (Resv). Endogenous VAMP7 was detected by indirect IF. As shown in **Figure 7A**, cells overexpressing GFP-vector and pSUPER BECN1^{KD} incubated under autophagic stimulation conditions presented a marked decrease in VAMP7-positive structures at the cell tips compared with untransfected cells or with cells co-expressing GFP-vector and the scrambled plasmid, incubated in the conditions mentioned above. The percentage of cells with VAMP7-positive structures at the cell periphery was determined (**Fig. 7B**). White and black bars indicate transfected and untransfected cells respectively in each condition studied.

We next analyzed the distribution of VAMP7 in MEF ATG5wt and MEF ATG5 knockdown cells incubated in the presence of autophagic stimulators. MEF cells were incubated in starvation media (Stv) or in complete media in the absence (Ctr) or presence of resveratrol (Resv). Endogenous VAMP7 and LC3 were detected by indirect IF. As expected, in MEF ATG5wt cells incubated in starvation media or with resveratrol, a fraction of LC3 and VAMP7-labeled vesicles redistributed at the cell edge. In contrast, in MEF ATG5$^{-/-}$ cells incubated in the same conditions mentioned above there were no VAMP7-labeled vesicles at the cell tips (**Fig. S5A and S5B**).

Taken together, these results indicate that two key proteins of the autophagy pathway (i.e., ATG5 and BECN1) are necessary for the autophagy-induced redistribution of VAMP7-positive structures toward the cell periphery.

Transport of VAMP7 structures to focal adhesions is microtubule dependent. In order to analyze if microtubule-disrupting agents or compounds that inhibit actin polymerization are able to impair the delivery of VAMP7 to the cell periphery upon starvation-induced autophagy we incubated cells in the presence of different inhibitors. HeLa cells were incubated in complete media or in starvation media in the absence or the presence of the microtubule depolymerizing agents vinblastin (Vb) or nocodazole (Noc) or with the actin filaments inhibitor latrunculin B (Lat). Subsequently, endogenous VAMP7 was detected by IF. As shown in **Figure 8A**, both Vb and Noc hampered the redistribution of VAMP7 to the cell periphery. In cells incubated in the presence of Lat, VAMP7 presented a perinuclear distribution, probably because this inhibitor caused cell detachment, generating rounded cells. To further analyze the effect of Vb in the transport of VAMP7 to the cell periphery, a population of cells was incubated with LysoTracker Red to label the lysosomes and then endogenous VAMP7 was detected (**Fig. 8B**). Endogenous M6PR and VAMP7 were also detected in another subset of cells. As shown in **Figure 8B**, cells incubated in the presence of Vb presented a marked decrease in LysoTracker Red labeled vesicles. Furthermore, an increased number of late endosomes labeled with VAMP7 and M6PR close to the perinuclear region was observed in cells treated with Vb.

We next assessed the effect of these agents on the transport of autophagosomes to focal adhesions. Endogenous LC3 and VAMP7 proteins were detected in HeLa cells incubated in complete media or in starvation media in the presence of Vb. As shown in **Figure 8C**, the microtubule depolymerizing agent hampered the transport of autophagosomes to the cell periphery. Taken together, these results suggest that microtubules are necessary for VAMP7-autophagosomes transport to the cell tips.

Proteins involved in microtubule-mediated trafficking participate in the transport of the VAMP7-vesicles. It has been shown that the RAB7 effector RILP (Rab interacting lysosomal protein) may coordinate the biogenesis of late endosomes via dynein-mediated motility.[31] To investigate the possible role of this effector in the transport of the VAMP7-labeled vesicles to the cell periphery, cells overexpressing GFP-RILP were incubated

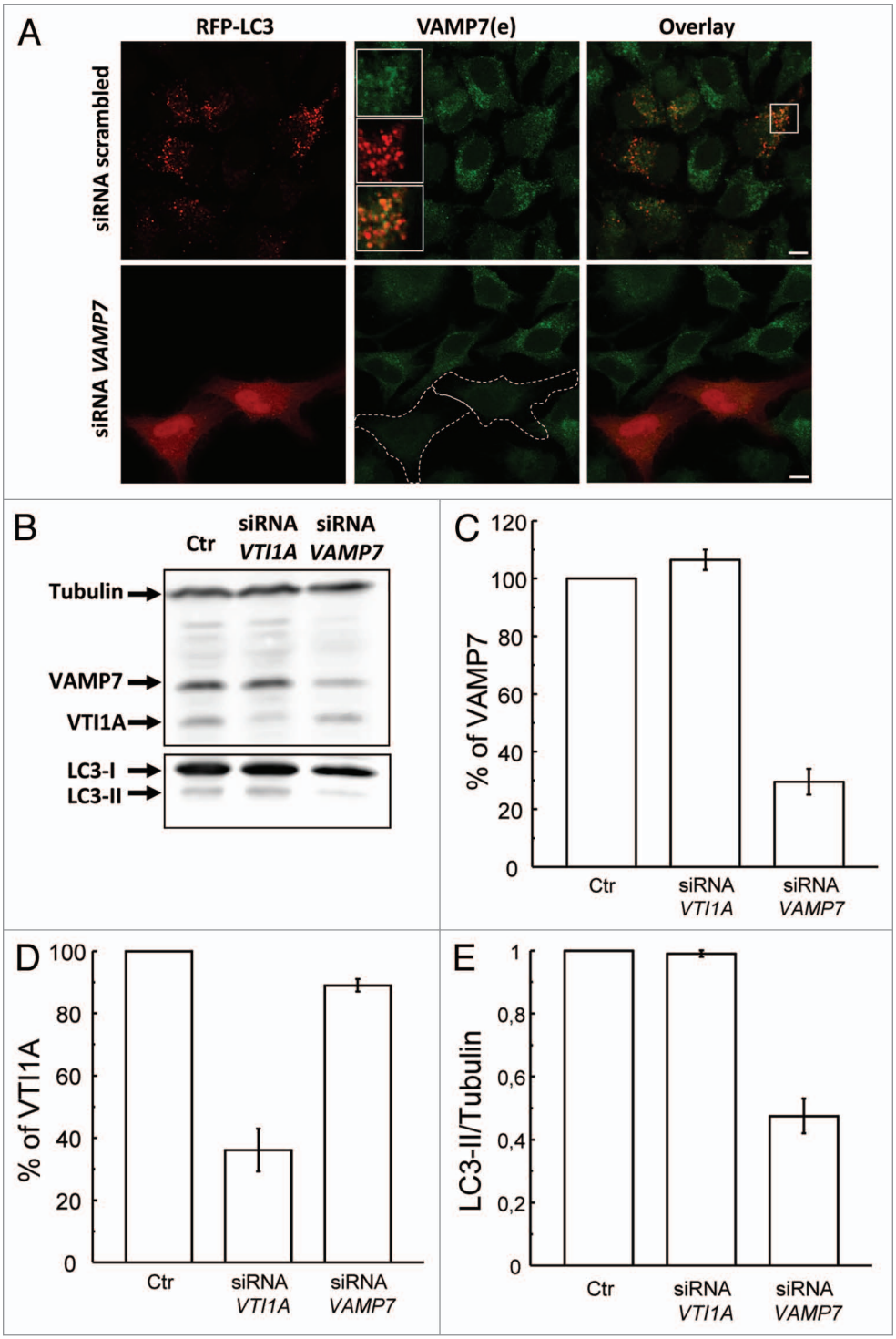

Figure 6. VAMP7 but not VTI1A is required to autophagosome formation. (**A**) HeLa cells were cotransfected with RFP-LC3 plasmid and a scrambled siRNA or a siRNA against *VAMP7*. Cells were fixed and VAMP7 was detected by indirect immunofluorescence. Images were obtained by confocal microscopy. Scale bars: 5 μm. (**B**) HeLa cells transfected with the scrambled siRNA (Ctr), siRNA against *VAMP7* or siRNA against *VTI1A* were lysed with 1% Triton X100 in PBS. Samples were subjected to SDS-PAGE and transferred onto a nitrocellulose membrane as described in Materials and Methods. The membrane was incubated with a rabbit anti-LC3, a mouse anti-VAMP7, mouse anti-VTI1A and the corresponding HRP-labeled secondary antibodies, and subsequently developed with an enhanced chemiluminescence detection kit. (**C and D**) The percentage of VAMP7 and VTI1A were quantified from images as the ones displayed in (**B**). (**E**) The LC3II/tubulin ratio was measured from images as those displayed in (**B**). Images are representative of two independent experiments.

in complete media or starvation and then VAMP7 was detected by IF. As shown in **Figure 9A**, transfected cells presented a perinuclear distribution of VAMP7 even in starvation conditions. In contrast, nontransfected cells showed the peripheral distribution of VAMP7 in starvation conditions as described above. The percentage of cells with VAMP7 at the cell periphery was quantified in **Figure 9B**. This result suggests that RILP favors the retrograde transport of VAMP7-positive vesicles from the focal adhesions to the perinuclear region.

Kinesin molecules are motor proteins capable of moving along microtubules by hydrolyzing ATP. KIF5 belongs to the kinesin superfamily of proteins (KIFs) which typically move toward the plus end of microtubules and participate in anterograde transport.[32] To analyze the role of KIF5 in the transport of VAMP7-vesicles to the cell periphery, HeLa cells were cotransfected with the GFP-vector and pcDNA-KIF5 wt or the dominant negative mutant pcDNA-KIF5T93N, which contain a mutation in the ATP-binding motif. Then, endogenous VAMP7 was detected in cells incubated in complete media or in an amino acid, serum-free media. As shown in **Figure 9C**, in cells overexpressing KIF5 wt and in nontransfected cells (**Fig. 9C, g–i**) presented VAMP7-vesicles at focal adhesions in starvation conditions. Moreover, we observed that in cells overexpressing KIF5 even incubated in control conditions, presented a peripheral distribution of VAMP7 (**Fig. 9C, d–f**), suggesting that the solely expression of KIF5 leads to the transport of the VAMP7-structures to the cell periphery. Interestingly, overexpression of the negative mutant KIF5T93N hampered the transport of VAMP7 to the focal adhesions (**Fig. 9C, m–o**). The percentage

of cells with VAMP7 positive structures at the cell periphery was quantified (**Fig. 9D**). Taken together, these results indicate that the kinesin KIF5 is necessary for the transport of the VAMP7-vacuoles to the cell edge.

The VAMP7-labeled structures at the cell periphery are loaded with ATP. As mentioned, VAMP7 is required for the fusion of MVBs with the plasma membrane to release exosomes into the extracellular medium.[18] Several cell types release ATP into the extracellular space in response to different stress conditions.[33] To determine whether ATP was present in the VAMP7-positive structures, we detected this nucleotide by labeling HeLa cells with quinacrine. Cells were incubated in starvation media (Stv) or in complete media in the absence (control, Ctr) or the presence of monensin (Mon). Monensin was used as a negative control because it produces a decreased fluorescence of quinacrine puncta.[34] Cells were incubated with 25 μM of quinacrine for 20 min to label vesicles containing ATP,[35-37] and then subjected to IF to detect endogenous VAMP7. As shown in **Figure 10A**, in control conditions very few VAMP7-positive vesicles were labeled by quinacrine (**Fig. 10A, a–c**). In contrast, an increased colocalization between both markers was observed in conditions that stimulate autophagy (**Fig. 10A, g–l**). Interestingly, in starvation conditions most of the VAMP7-positive structures containing ATP were localized at the cell periphery. The percentage of colocalization (**Fig. 10B**) and the percentage of cells with ATP/VAMP7-labeled vesicles (**Fig. 10C**) were quantified. As shown in **Figure 10D**, the Pearson's coefficient in starvation conditions is over 0.5, indicating that there is a marked colocalization between VAMP7 and quinacrine in this condition. These results indicate that induction of autophagy by starvation causes an increased number of ATP-containing vesicles labeled with VAMP7 and, in addition, a redistribution of these vesicles toward the cell periphery.

ATP-loaded amphisomes fuse with plasma membrane upon incubation in starvation conditions. TIRF on a rapid time scale was next used to visualize events in proximity to the cell membrane. This microscopy method was performed to address whether the ATP-loaded autophagic vacuoles were able to fuse with the plasma membrane releasing the nucleotide into the extracellular space. Cells were transiently transfected with RFP-LC3 and autophagy was induced by starvation media for 6 h. Cells were incubated with 25 μM of quinacrine for 20 min to label vesicles containing ATP. By TIRF microscopy we were able to observe the fusion of RFP-LC3 positive vesicles containing ATP (i.e., amphisomes) with the plasma membrane

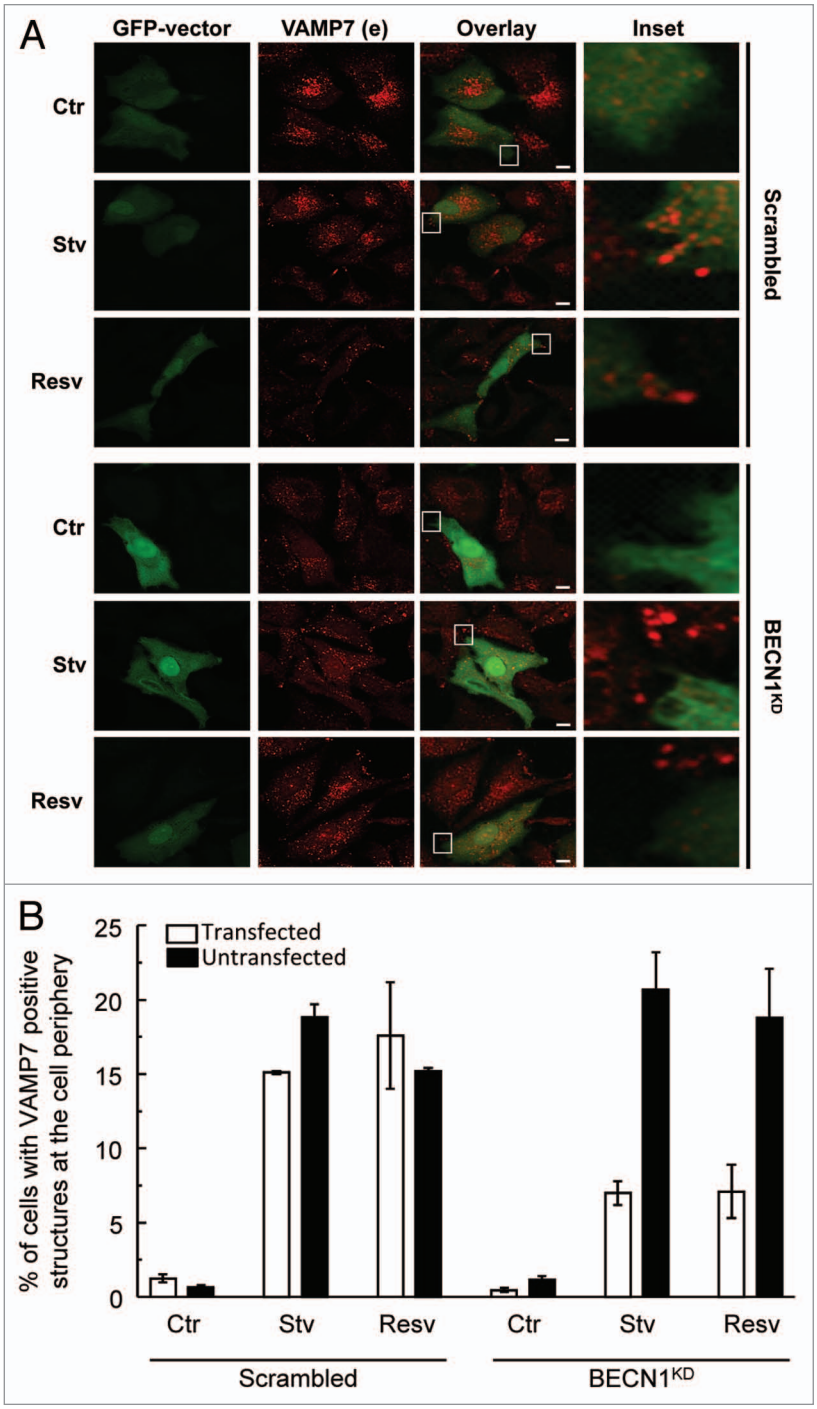

Figure 7. BECN1 is necessary for autophagy-induced transport of VAMP7 structures to focal adhesions. (**A**) HeLa cells were cotransfected with a GFP-Vector plasmid and a pSUPER scrambled or a pSUPER BECN1^{KD}. Cells were incubated for 4 h in starvation media (Stv) or 3 h in complete media in absence (Ctr) or presence of resveratrol (Resv). Then, cells were fixed and VAMP7 was detected by indirect immunofluorescence. Images were obtained by confocal microscopy. Scale bars: 5 μm. (**B**) The percentage of cells with VAMP7-positive structures at the cell periphery were quantified from images as the ones displayed in (**A**). White and black bars indicates transfected and untransfected cells respectively in each condition studied and represent the mean ± SEM of two independent experiments. At least 100 cells were counted in each condition.

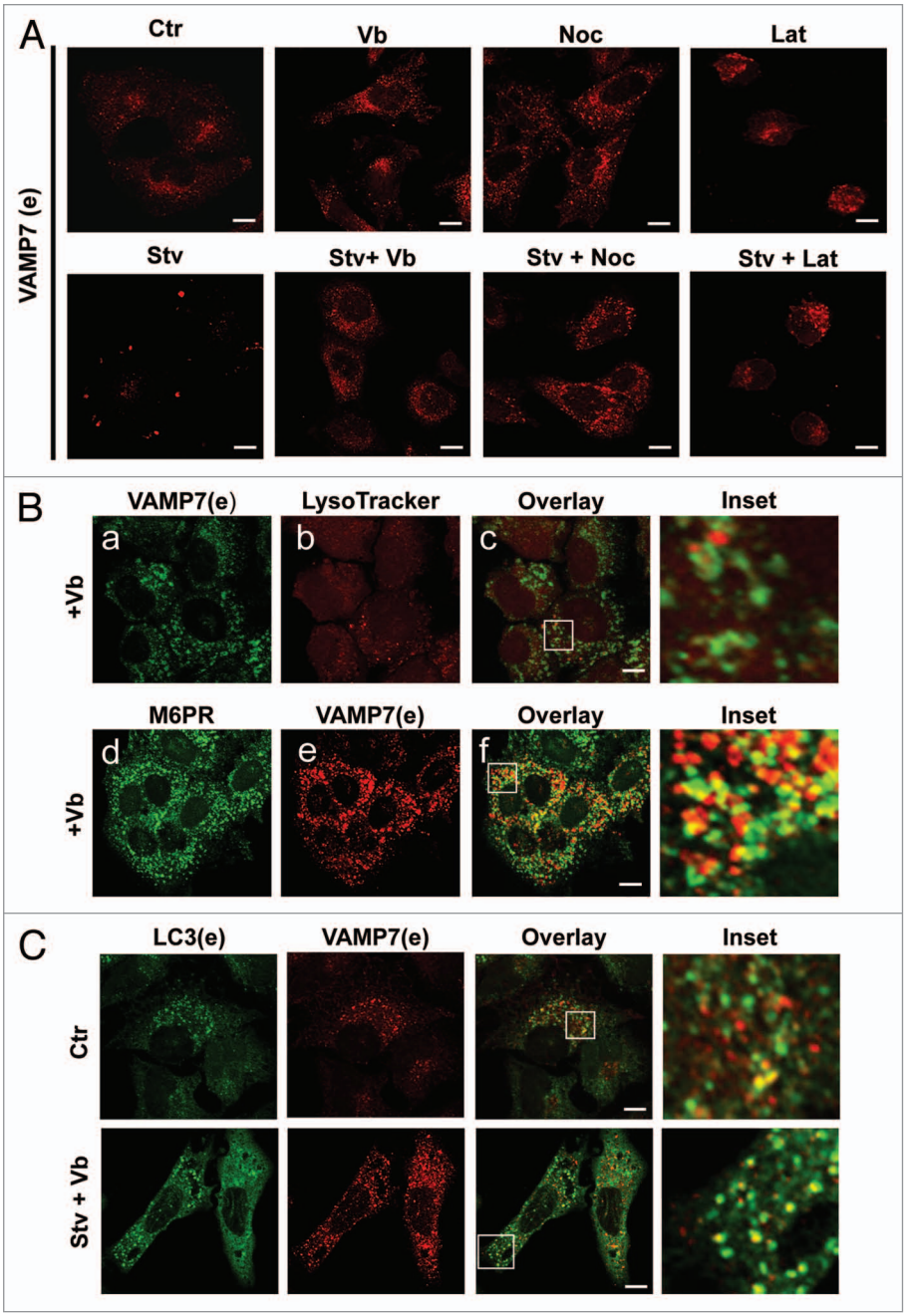

Figure 8. Vinblastin impairs the VAMP7 redistribution at the focal adhesions induced by starvation. (**A**) HeLa cells were incubated in complete media or in starvation media in the absence or the presence of latrunculin B (Lat), vinblastin (Vb) or nocodazole (Noc). Endogenous Vamp7 was detected by indirect immunofluorescence (IF). (**B**) Hela cells were incubated in the presence of vinblastin (Vb). A population of cells was incubated with LysoTracker Red (upper panel) to label the lysosomes. Endogenous VAMP7 (lower panel) was detected by indirect IF (green). In another subset of cells, endogenous M6PR and VAMP7 were detected by indirect IF. (**C**) HeLa cells were incubated in complete media or in starvation media in the presence of Vb. Endogenous LC3 and VAMP7 proteins were detected by indirect IF. Images were obtained by confocal microscopy. Scale bars: 5 μm.

(**Movie 1; Fig. 11A**). This was visualized as rapid, simultaneous diffusion of RFP-LC3 and quinacrine into the plasma membrane. Whereas the size of the fluorescent area increased with time, indicating the fusion of the vesicle at the cell surface (squares), the fluorescence intensity of the vesicle at the exocytic site show a rapid rise followed by a decrease to background levels (**Fig. 11B**, diamonds).

To address whether autophagy stimulation by starvation or resveratrol leads to ATP release, we quantified the amount of this nucleotide in the extracellular medium of cultured cells. HeLa cells were grown to confluence in a 6-well plate and washed with PBS. Cells were incubated at 37°C in amino acid and serum-free media (Stv) or in full nutrient (Ctr) in presence or absence of resveratrol (resv). A 50 μl aliquot of the media was collected every 30 min and the released ATP was determined by a chemiluminescent assay (see Materials and Methods). Interestingly, our result shows that in starvation conditions there was an increased level of ATP released into the extracellular space, which was even higher in the presence of resveratrol (**Fig. 11C**). Taken together these results clearly indicate that amphisomes loaded with ATP can fuse with the plasma membrane releasing the nucleotide into the extracellular medium.

Discussion

In the present report, we present evidence that in HeLa and other cancer cell lines, VAMP7 participates in the transport of autophagosomes to the cell periphery. Our results indicate that upon autophagy induction a population of VAMP7-structures also labeled by LC3 redistributed at the tips of the cell. This suggests that autophagic stimulators such as starvation media, rapamycin, resveratrol or spermidine can modulate the distribution of some endocytic/autophagic compartments to the cell periphery. Interestingly, a recent publication has demonstrated that trypomastigotes infection in HeLa cells incubated in starvation generated a dispersed localization at the cellular edge of lysosomes and increased exocytosis.[38]

We have demonstrated that in cells incubated in starvation media, those VAMP7-positive vacuoles colocalized with the focal adhesion markers PXN and VCL. Previous studies have shown that VAMP7 is required to matrix metalloproteinase (MT1-MMP)-dependent matrix degradation at invadopodia, maintaining the functional machinery required for cancer cell invasion.[39] These results are supported by a recent

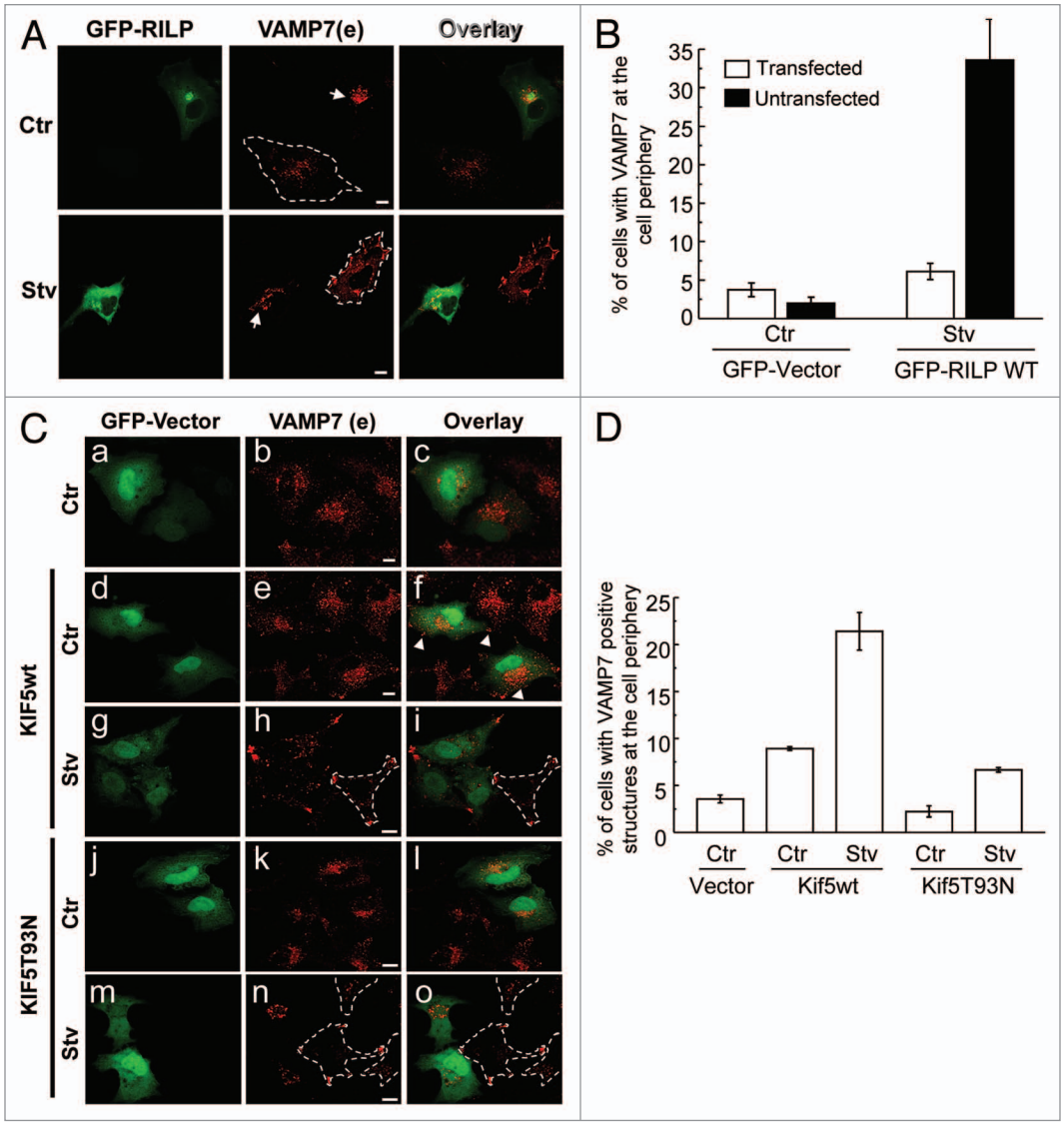

Figure 9. VAMP7-positive vesicles are transported by proteins involved in microtubule-mediated trafficking. (**A**) HeLa cells overexpressing GFP-RILP were incubated for 4 h in complete media or starvation. Endogenous VAMP7 was detected by indirect immunofluorescence (IF). Scale bars: 5 μm. Arrows: VAMP7 structures localized at the perinuclear region. (**B**) The percentage of cells with VAMP7 at the cell periphery was quantified from images as those displayed in (**A**) and represent the mean ± SEM of two independent experiments. At least 50 cells were counted in each condition. (**C**) HeLa cells co-transfected with GFP-vector and pcDNA-Kif5 wt or pcDNA-Kif5T93N were incubated for 4h in complete media or in an amino acid, serum-free media. Endogenous VAMP7 was detected by indirect IF. Arrows: VAMP7 structures localized at the cell tips. Scale bars: 5 μm. Images were obtained by confocal microscopy. (**D**) The percentage of cells with VAMP7 positive structures at the cell periphery was quantified from images as those displayed in (**C**) and represent the mean ± SEM of two independent experiments.

paper in which it has been shown that VAMP7 mRNA is present in pseudopodia of murine fibroblasts in response to migratory stimuli, suggesting that migrating cells probably synthesize VAMP7 in pseudopodia.[40] Interestingly, experiments performed in HeLa cells have demonstrated that the molecular composition of ECM modulates autophagy and its role in cell survival during starvation.[41] Thus, autophagy probably has an important role in cell-matrix interaction throughout the fusion of amphisomes with the plasma membrane at the cell edge.

We have also observed that overexpression of the N-terminal domain of TI-VAMP/VAMP7, which inhibits SNARE complex formation,[42] caused a marked decrease in the redistribution toward the cell periphery of endogenous VAMP7-labeled vesicles. Likewise, knockdown of VAMP7 affected the distribution of LC3-positive vesicles at the cell periphery, altering autophagosome formation. Our results are consistent with previous observations indicating the requirement for VAMP7 in autophagosome biogenesis.[20] In addition, we have demonstrated that this redistribution toward the cell periphery upon autophagy induction was dependent on the autophagic proteins ATG5 and BECN1. Interestingly, these VAMP7-labeled structures localized at the focal adhesions upon starvation stimuli were not substantially marked by CTSD or LAMP1, suggesting that the VAMP7 structures localized at focal adhesions are not lysosomes

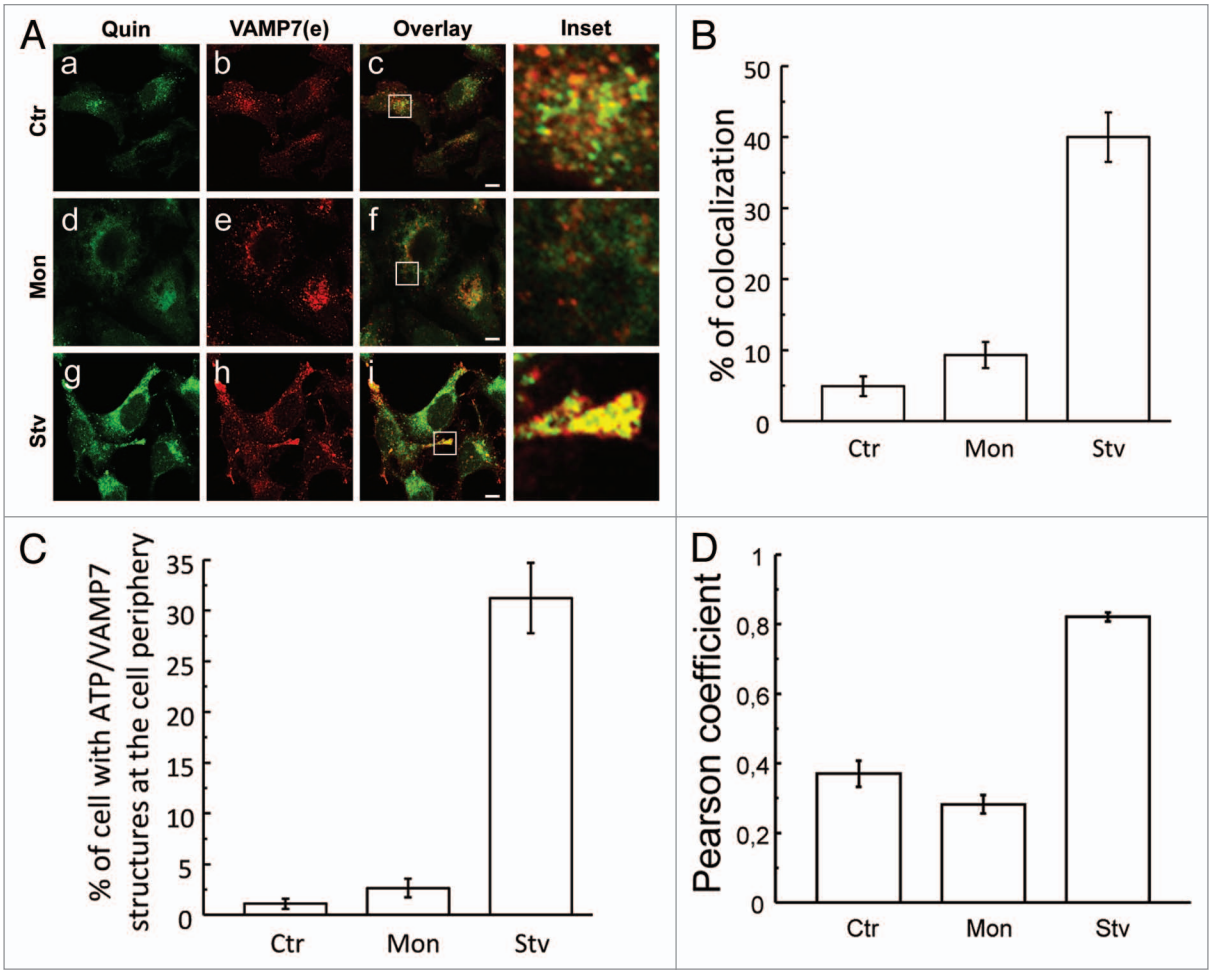

Figure 10. Starvation caused an increased number of ATP-loaded vesicles labeled with VAMP7 at the cell periphery. (**A**) HeLa cells were incubated in starvation media (Stv) or in complete media in the absence (Ctr) or presence of monensin (Mon). Afterwards, cells were incubated with 25 μM of quinacrine (Quin) for 20 min and subjected to indirect immunofluorescence to detect endogenous VAMP7. Images were obtained by confocal microscopy. Scale bars: 5 μm. The percentage of colocalization (**B**) and the percentage of cells with ATP/VAMP7-labeled vesicles at the cell periphery (**C**) were quantified from images as those displayed in (**A**). At least 100 cells were counted in each condition.

or autolysosomes. This observation is consistent with previous reports showing that in cells incubated in starvation conditions the proportion of perinuclear lysosomes increased.[43] We present evidence that the VAMP7-positive autophagosomes at focal adhesions were labeled by overexpressed GFP-Rab7. There was also a marked colocalization between the M6P receptor (late endosome marker) and VAMP7 in cells incubated in starvation media, supporting the conclusion that the autophagic vacuoles localized at the focal adhesions are amphisomes. In addition, we have shown that the redistribution of amphisomes to focal adhesions upon starvation was completely abrogated by microtubule depolymerizing agents, suggesting that microtubules are necessary for this transport to the cell periphery.

The small GTP-binding protein RAB7 mediates its function in part by the RAB7 effector RILP (Rab interacting lysosomal protein). It has been shown that the RAB7 effector RILP may coordinate the biogenesis of late endosomes via dynein-mediated motility.[31] We have shown that overexpressed GFP-RILP produces an accumulation of VAMP7 structures at the peri-nuclear region. Interestingly, in cells overexpressing GFP-RILP incubated in starvation media, VAMP7 positive structures were not able to distribute peripherally. These data indicate that RILP transports the amphisomes via the microtubules in centripetal direction. This result is in agreement with previous studies showing that RILP regulates microtubule minus-end directed transport[44,45] and connect phagosomes with dynein-dynactin (a microtubule-associated motor complex), displacing phagosomes to the perinuclear region.[46] Interestingly, Jordens et al. have shown that overexpression of a dominant-negative mutant of RILP impairs the recruitment of the dynein/dynactin complex, resulting in the relocation of late endosomal structures toward the cell periphery by a kinesin dependent event.[47]

As mentioned above, kinesin superfamily proteins (KIFs) participate in anterograde transport and move the cargo toward the plus end of microtubules. Previous studies have demonstrated that two motor proteins, KIF1B and KIF2, redistribute lysosomes to the cell periphery.[47-49] Our data indicate that cells overexpressing KIF5 wt presented a redistribution VAMP7-structures

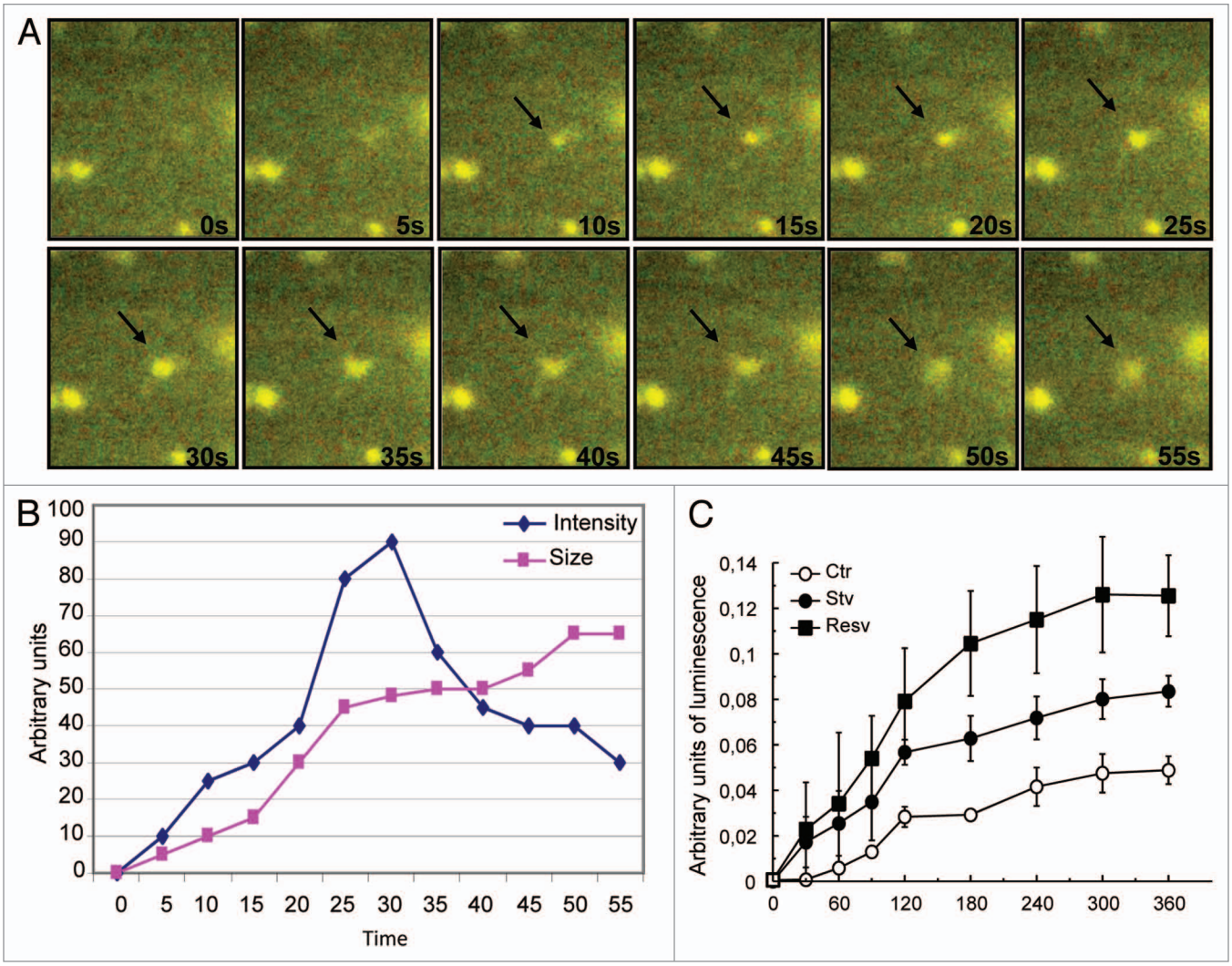

Figure 11. TIRF analyses of exocytic events in transfected HeLa cells. Cells were transiently transfected with RFP-LC3 (red) and autophagy was induced by starvation media for 6 h. Cells were incubated with 25 μM of quinacrine for 20 min (green). (**A**) Time in seconds corresponding to each frame is indicated. Arrows indicate the exocytic site on the cell surface. (**B**) The fluorescence intensity (diamonds) and the size (squares) of the LC3 and quinacrine-positive structure were quantified from the image displayed in (**A**). (**C**) HeLa cells were grown to confluence in 6-well plate. Cells were washed with PBS and incubated at 37°C in amino acid and serum-free media (Stv) or in full nutrient (Ctr) in the presence or absence of resveratrol (Resv). Aliquots of the culture media (50 μl) were collected every 30 min for 6 h and incubated with 50 μl firefly luciferin–luciferase as described in Materials and Methods. ATP dependent chemiluminescence activity of the media samples was measured in constant darkness using a luminometer.

at the cell tips in control condition, indicating that the solely expression of the kinesin KIF5 is necessary for the transport of the VAMP7-structures to the cell periphery. Consistently, overexpression of an ATP-defective mutant of KIF5 hampered the transport of VAMP7 to the focal adhesions even in starvation conditions. These observations indicate that KIF5 is necessary for the redistribution of VAMP7-positive structures at the focal adhesions upon starvation. Consistently, results obtained in Dr. Rubinsztein's laboratory indicate that nutrients modulate lysosomal movement affecting the binding of proteins such as KIF2 and ARL8B to lysosomes and microtubules.[43] On the other hand, a recent paper has revealed that depletion of the RAB7 effector FYCO1, which also binds ATG8 (i.e., LC3), leads to perinuclear accumulation of autophagosomes.[50] Interestingly, a proteomic analysis of the autophagy interaction network in human cells has established that depletion of KIF5B causes to peri-nuclear accumulation of autophagosomes, suggesting that FYCO1-positive autophagosomes binds to microtubules throughout KIF5B to maintain cortical localization.[51] On the other hand, Ravikumar and colaborators have shown that plasma membrane contribute to the formation of phagophore assembly sites.[52] However, our results indicate that in cells overexpressing the ATP mutant of KIF5 which produce a perinuclear redistribution of the VAMP7-positive autophagosomes, no VAMP7-positive amphisomes were localized at the tips of the cell in starvation condition, suggesting that the plasma membrane does not substantially supply membrane to form this particular type of structures.

A response to different stress conditions in several cell types is a regulated release of ATP into the extracellular space.[33] Previous studies have demonstrated that ATP is released via vesicular

exocytosis in astrocytes.[35,37,53] We have observed in a mammalian tumor cell line that VAMP7-positive autophagosomes, which contain ATP, are redistributed toward focal adhesions upon physiological stress conditions (i.e., starvation). We propose that these ATP-containing vesicles fuse with the plasma membrane to release their content in the extracellular space upon autophagy activation. Extracellular ATP released from stressed cells is one of the most pleiotropic activators of the NLRP3 inflammasome,[54] driving the secretion of interleukin-1β.[55,56] Furthermore, extracellular ATP is recognized as an important autocrine/paracrine signal molecule that participates in the regulation of several cellular functions.[57-61] Interestingly, ATP is released from dying tumor cells by exposure to several cell death inducers.[55,62] Recent studies have identified tumor-derived ATP as a new damage-associated molecular pattern, being necessary for cancer cell death to be immunogenic.[55] On the other hand, a very recent publication from Dr. Kroemer's lab has shown that autophagy is necessary for the immunogenic release of ATP from dying cells, and that the increased level of extracellular ATP favors the efficacy of antineoplastic chemotherapies when autophagy is disabled.[63]

To summarize, the data presented here demonstrate for the first time the molecular machinery required for fusion of the ATP-loaded autophagic with the plasma membrane, to release this nucleotide into the extracellular medium upon autophagy stimulation. Although the physiological relevance of this mechanism is poorly understood, several studies have associated the ATP released to the extracellular space with processes like immunogenicity of cancer cell death or inflammation. Further studies will be necessary to elucidate the physiological importance of the distribution of ATP-loaded amphisomes toward the cell periphery in a cell stress situation such as starvation.

Materials and Methods

Materials. DMEM medium was obtained from Gibco (Invitrogen, 11965-175) and fetal bovine serum (FBS) from Natocor (SFBE). The Earle's Balanced Salts Solution, EBSS (starvation) media and Vinblastine are from Sigma (E7510, V1377). LysoTracker Red was obtained from Invitrogen (L7528). Quinacrine mustard dihydrochloride was obtained from Sigma (Q2876). Endogenous VAMP7 was detected with a mouse anti-SYBL1 (Abcam, ab36195). Rabbit anti-CTSD was kindly provided by Dr. Maximiliano Gutierrez (Helmholtz Centre for Infection Research). Mouse anti-VTI1A was from BD (611220).

Plasmids. The pEGFP-LC3wt was kindly provided by Dr. Noboru Mizushima (Tokyo Medical and Dental University). pRFP-LC3 was subcloned as indicate in our recent publication.[18] pEGFPC3 encoding GFP-TI-VAMP or the GFP-Longin domain was kindly provided by Dr. Thierry Galli (Institut Jacques Monod) and have been described previously.[64] The plasmid pEGFP- RAB7wt was a generous gift from Bo van Deurs (University of Copenhagen). The pCDNA KIF5wt, pCDNA KIF5T93N was kindly provided by Dr. Alfredo Caceres (Mercedes and Martín Ferreyra Institute). pEGFP-VCL, pEGFP-PXN was a gift from Carlos Arregui (Universidad de San Martín). The plasmids encoding enhanced GFP (EGFP)-RAB5wt was kindly provided by Dr. Philip D. Stahl (Washington University). The pEGFP-RILP was kindly provided by Dr. Mauricio Terebiznik (Hospital for Sick Children). The pSUPER.retro.puro vector BECN1 knock down (KD) was kindly provided by Dr. William A. Maltese (Medical University of Ohio).

SH2 cell culture and transfection. HeLa cells were grown in DMEM 10% FBS (full nutrient medium), streptomycin (50 μg/ml) and penicillin (50 U/ml) at 37°C in an atmosphere of 95% air and 5% CO_2. For some experiments cells were incubated in starvation media EBSS. For specific experiments HeLa cells were transiently transfected with pEGFP-Vector, pEGFP-VCL, pEGFP-PXN, pEGFP- RAB5wt, pEGFP-LAMP1, pEGFP-VAMP7, pEGFP-NT-VAMP7, pEGFP-RAB7wt, pEGFP-RILP, pCDNA KIF5wt, pCDNA KIF5T93N or co-transfected with pEGFP-RAB7wt/pRFP-LC3 and pEGFP-RAB7wt/pRFP-LC3, using LipofectAMINE 2000 (Invitrogen, 11668-019) as indicated by the manufacturer.

Indirect immunofluorescence. HeLa cells were fixed with 0.5 ml of 3% paraformaldehyde solution in PBS for 10 min at room temperature, washed with PBS and quenched with NH_4Cl 50 mM in PBS for 20 min. Then, cells were permeabilized with 1% saponin in PBS containing 1% BSA (blocking buffer). After blocking, cells were incubated with the indicated primary antibodies for 1 h. Cells were washed three times in blocking buffer and subsequently incubated for 1 h with the indicated fluorophore-conjugated secondary antibody. Endogenous LC3 was detected with a rabbit monoclonal anti-LC3 (dilution 1:50). Endogenous VAMP7 was detected with the mouse monoclonal anti-SYBL1 (dilution 1:100) and cathepsin D was detected with a rabbit anti-CTSD (1:50). Endogenous VTI1A was detected with a mouse monoclonal anti-VTI1A (dilution 1:300) whereas M6PR was detected with a rabbit anti-M6PR (1:100). Bound antibodies were subsequently detected by incubation with Cy3 goat-anti-mouse secondary antibody (dilution 1:600, Jackson ImmunoResearch, 115-166-003) and Alexa Fluor 488-labeled goat anti-rabbit secondary antibody (dilution 1:500, Molecular Probes, A-11008). Coverslips were mounted on glass slides using Mowiol and examined by fluorescence confocal microscopy.

siRNA-mediated VAMP7 or VTI1A "knockdown". Short interfering RNA directed to human VAMP7 (241467) or VTI1A (37855) were purchased from Ambion. siRNA (final concentration 10 μM) were mixed with LipofectAMINE 2000 (Invitrogen, 11668-019) as indicated by the manufacturer. The mixture was then added directly to HeLa cells (1×10^5/ml) in DMEM cell culture medium without serum. Cells were analyzed at 72 h post-transfection and endogenous VAMP7, VTI1A and LC3 were detected by western blot.

Fluorescence microscopy. HeLa cells transfected with the different plasmids were analyzed by confocal microscopy using a Olympus Confocal Microscope FV1000-EVA (Olympus). Images were processed using Adobe CS (Adobe Systems), ImageJ software, Metamorph Program, serie 4.5 (Universal Images Corporation) and FV10-ASW program (Olympus).

SDS-PAGE and western blot. Samples of the total cell pellet (100 μg protein) were solubilized in reducing SDS loading

buffer and incubated for 5 min at 95°C. Samples were run on 12,5% polyacrylamide gels and transferred to Hybond-ECL (Amersham) nitrocellulose membranes. The membranes were blocked for 1 h in Blotto (5% nonfat milk, 0.1% Tween 20 and PBS), washed twice with PBS and incubated with primary antibodies and peroxidase-conjugated secondary antibodies. The corresponding bands were detected using an enhanced chemiluminescence detection kit from Pierce (Tecnolab S.A.).

TIRF images of quinacrine and RFP-LC3 were obtained with a PlanApo × 100 (NA 1.42) objective mounted on an Olympus FV1000-EVA, equipped with a 12-bit digital charge-coupled device camera (Hamamatsu Photonics) and controlled by the μManager software 1.4 (Vale Lab, UCSF).[65] Intraobjective TIRF was obtained with 473-nm and 559-nm laser through a EVA module incorporated in Olympus FW10-ASW 1.7 software.

Measurement of ATP release. ATP in the samples was measured by a luciferase–luciferin-based assay, using ATP Assay Mix and ATP Assay Mix Dilution Buffer supplied by Sigma-Aldrich and following the manufacturer's instructions. HeLa cells were grown to confluence in 35-mm Petri dishes. After washing with PBS, cells were incubated at 37°C in amino acid and serum-free media or in full nutrient in the presence or absence of 100 μM of resveratrol. Supernatant aliquots of 50 μl were collected every 30 min for 6 h and incubated with 50 μl firefly luciferin–luciferase (Sigma, FLAAM-5VL) in a 96-well black plate. The ATP-dependent chemiluminescent activity was measured in constant darkness using a luminometer Fluorocount Ascent (Thermo, 1506450).

Statistical analysis. Results are presented as the mean ± SEM from at least two independent experiments. The comparisons were performed using ANOVA in conjunction with Tuckey and Dunnett tests. Significant differences: *$p < 0.01$; **$p < 0.005$.

Disclosure of Potential Conflicts of Interest

No potential conflicts of interest were disclosed.

Acknowledgments

We thank Dr. Luis Mayorga for critical reading of this manuscript. We also thank Alejandra Medero for technical assistance with tissue culture. This work was partly supported by grants from Agencia Nacional de Promoción Científica y Tecnológica (PICT 2005 38420 and PICT 2008 0192), SeCTyP (Universidad Nacional de Cuyo) to M.I.C.

Supplemental Materials

Supplemental materials may be found here:
www.landesbioscience.com/journals/autophagy/article/21858

References

1. Knecht E, Aguado C, Cárcel J, Esteban I, Esteve JM, Ghislat G, et al. Intracellular protein degradation in mammalian cells: recent developments. Cell Mol Life Sci 2009; 66:2427-43; PMID:19399586; http://dx.doi.org/10.1007/s00018-009-0030-6
2. Cuervo AM. The plasma membrane brings autophagosomes to life. Nat Cell Biol 2010; 12:735-7; PMID:20680002; http://dx.doi.org/10.1038/ncb0810-735
3. Hailey DW, Rambold AS, Satpute-Krishnan P, Mitra K, Sougrat R, Kim PK, et al. Mitochondria supply membranes for autophagosome biogenesis during starvation. Cell 2010; 141:656-67; PMID:20478256; http://dx.doi.org/10.1016/j.cell.2010.04.009
4. Hayashi-Nishino M, Fujita N, Noda T, Yamaguchi A, Yoshimori T, Yamamoto A. A subdomain of the endoplasmic reticulum forms a cradle for autophagosome formation. Nat Cell Biol 2009; 11:1433-7; PMID:19898463; http://dx.doi.org/10.1038/ncb1991
5. Mari M, Griffith J, Rieter E, Krishnappa L, Klionsky DJ, Reggiori F. An Atg9-containing compartment that functions in the early steps of autophagosome biogenesis. J Cell Biol 2010; 190:1005-22; PMID:20855505; http://dx.doi.org/10.1083/jcb.200912089
6. van der Vaart A, Reggiori F. The Golgi complex as a source for yeast autophagosomal membranes. Autophagy 2010; 6:800-1; PMID:20714226; http://dx.doi.org/10.4161/auto.6.6.12575
7. Yen WL, Shintani T, Nair U, Cao Y, Richardson BC, Li Z, et al. The conserved oligomeric Golgi complex is involved in double-membrane vesicle formation during autophagy. J Cell Biol 2010; 188:101-14; PMID:20065092; http://dx.doi.org/10.1083/jcb.200904075
8. Ylä-Anttila P, Vihinen H, Jokitalo E, Eskelinen EL. 3D tomography reveals connections between the phagophore and endoplasmic reticulum. Autophagy 2009; 5:1180-5; PMID:19855179; http://dx.doi.org/10.4161/auto.5.8.10274
9. Zoppino FC, Militello RD, Slavin I, Alvarez C, Colombo MI. Autophagosome formation depends on the small GTPase Rab1 and functional ER exit sites. Traffic 2010; 11:1246-61; PMID:20545908; http://dx.doi.org/10.1111/j.1600-0854.2010.01086.x
10. Ravikumar B, Moreau K, Rubinsztein DC. Plasma membrane helps autophagosomes grow. Autophagy 2010; 6:1184-6; PMID:20861674; http://dx.doi.org/10.4161/auto.6.8.13428
11. Berg TO, Fengsrud M, Strømhaug PE, Berg T, Seglen PO. Isolation and characterization of rat liver amphisomes. Evidence for fusion of autophagosomes with both early and late endosomes. J Biol Chem 1998; 273:21883-92; PMID:9705327; http://dx.doi.org/10.1074/jbc.273.34.21883
12. Eskelinen EL. Maturation of autophagic vacuoles in Mammalian cells. Autophagy 2005; 1:1-10; PMID:16874026; http://dx.doi.org/10.4161/auto.1.1.1270
13. Chaineau M, Danglot L, Galli T. Multiple roles of the vesicular-SNARE TI-VAMP in post-Golgi and endosomal trafficking. FEBS Lett 2009; 583:3817-26; PMID:19837067; http://dx.doi.org/10.1016/j.febslet.2009.10.026
14. Brunger AT, Weninger K, Bowen M, Chu S. Single-molecule studies of the neuronal SNARE fusion machinery. Annu Rev Biochem 2009; 78:903-28; PMID:19489736; http://dx.doi.org/10.1146/annurev.biochem.77.070306.103621
15. Galli T, Zahraoui A, Vaidyanathan VV, Raposo G, Tian JM, Karin M, et al. A novel tetanus neurotoxin-insensitive vesicle-associated membrane protein in SNARE complexes of the apical plasma membrane of epithelial cells. Mol Biol Cell 1998; 9:1437-48; PMID:9614185
16. Advani RJ, Bae HR, Bock JB, Chao DS, Doung YC, Prekeris R, et al. Seven novel mammalian SNARE proteins localize to distinct membrane compartments. J Biol Chem 1998; 273:10317-24; PMID:9553086; http://dx.doi.org/10.1074/jbc.273.17.10317
17. Advani RJ, Yang B, Prekeris R, Lee KC, Klumperman J, Scheller RH. VAMP-7 mediates vesicular transport from endosomes to lysosomes. J Cell Biol 1999; 146:765-76; PMID:10459012; http://dx.doi.org/10.1083/jcb.146.4.765
18. Fader CM, Sánchez DG, Mestre MB, Colombo MI. TI-VAMP/VAMP7 and VAMP3/cellubrevin: two v-SNARE proteins involved in specific steps of the autophagy/multivesicular body pathways. Biochim Biophys Acta 2009; 1793:1901-16; PMID:19781582; http://dx.doi.org/10.1016/j.bbamcr.2009.09.011
19. Oishi Y, Arakawa T, Tanimura A, Itakura M, Takahashi M, Tajima Y, et al. Role of VAMP-2, VAMP-7, and VAMP-8 in constitutive exocytosis from HSY cells. Histochem Cell Biol 2006; 125:273-81; PMID:16195891; http://dx.doi.org/10.1007/s00418-005-0068-y
20. Moreau K, Ravikumar B, Renna M, Puri C, Rubinsztein DC. Autophagosome precursor maturation requires homotypic fusion. Cell 2011; 146:303-17; PMID:21784250; http://dx.doi.org/10.1016/j.cell.2011.06.023
21. Braun V, Fraisier V, Raposo G, Hurbain I, Sibarita JB, Chavrier P, et al. TI-VAMP/VAMP7 is required for optimal phagocytosis of opsonised particles in macrophages. EMBO J 2004; 23:4166-76; PMID:15470500; http://dx.doi.org/10.1038/sj.emboj.7600427
22. Pryor PR, Mullock BM, Bright NA, Lindsay MR, Gray SR, Richardson SC, et al. Combinatorial SNARE complexes with VAMP7 or VAMP8 define different late endocytic fusion events. EMBO Rep 2004; 5:590-5; PMID:15133481; http://dx.doi.org/10.1038/sj.embor.7400150
23. Ward DM, Pevsner J, Scullion MA, Vaughn M, Kaplan J. Syntaxin 7 and VAMP-7 are soluble N-ethylmaleimide-sensitive factor attachment protein receptors required for late endosome-lysosome and homotypic lysosome fusion in alveolar macrophages. Mol Biol Cell 2000; 11:2327-33; PMID:10888671
24. Kabeya Y, Mizushima N, Ueno T, Yamamoto A, Kirisako T, Noda T, et al. LC3, a mammalian homologue of yeast Apg8p, is localized in autophagosome membranes after processing. EMBO J 2000; 19:5720-8; PMID:11060023; http://dx.doi.org/10.1093/emboj/19.21.5720

25. Mauthe M, Jacob A, Freiberger S, Hentschel K, Stierhof YD, Codogno P, et al. Resveratrol-mediated autophagy requires WIPI-1-regulated LC3 lipidation in the absence of induced phagophore formation. Autophagy 2011; 7:1448-61; PMID:22082875; http://dx.doi.org/10.4161/auto.7.12.17802
26. Morselli E, Mariño G, Bennetzen MV, Eisenberg T, Megalou E, Schroeder S, et al. Spermidine and resveratrol induce autophagy by distinct pathways converging on the acetylproteome. J Cell Biol 2011; 192:615-29; PMID:21339330; http://dx.doi.org/10.1083/jcb.201008167
27. Madeo F, Eisenberg T, Büttner S, Ruckenstuhl C, Kroemer G. Spermidine: a novel autophagy inducer and longevity elixir. Autophagy 2010; 6:160-2; PMID:20110777; http://dx.doi.org/10.4161/auto.6.1.10600
28. Berrier AL, Yamada KM. Cell-matrix adhesion. J Cell Physiol 2007; 213:565-73; PMID:17680633; http://dx.doi.org/10.1002/jcp.21237
29. Gutierrez MG, Vázquez CL, Munafó DB, Zoppino FC, Berón W, Rabinovitch M, et al. Autophagy induction favours the generation and maturation of the Coxiella-replicative vacuoles. Cell Microbiol 2005; 7:981-93; PMID:15953030; http://dx.doi.org/10.1111/j.1462-5822.2005.00527.x
30. Jäger S, Bucci C, Tanida I, Ueno T, Kominami E, Saftig P, et al. Role for Rab7 in maturation of late autophagic vacuoles. J Cell Sci 2004; 117:4837-48; PMID:15340014; http://dx.doi.org/10.1242/jcs.01370
31. Progida C, Malerød L, Stuffers S, Brech A, Bucci C, Stenmark H. RILP is required for the proper morphology and function of late endosomes. J Cell Sci 2007; 120:3729-37; PMID:17959629; http://dx.doi.org/10.1242/jcs.017301
32. Xie P. Mechanism of processive movement of monomeric and dimeric kinesin molecules. Int J Biol Sci 2010; 6:665-74; PMID:21060728; http://dx.doi.org/10.7150/ijbs.6.665
33. Luna C, Li G, Qiu J, Challa P, Epstein DL, Gonzalez P. Extracellular release of ATP mediated by cyclic mechanical stress leads to mobilization of AA in trabecular meshwork cells. Invest Ophthalmol Vis Sci 2009; 50:5805-10; PMID:19608543; http://dx.doi.org/10.1167/iovs.09-3796
34. Miller DS, Villalobos AR, Pritchard JB. Organic cation transport in rat choroid plexus cells studied by fluorescence microscopy. Am J Physiol 1999; 276:C955-68; PMID:10199828
35. Coco S, Calegari F, Pravettoni E, Pozzi D, Taverna E, Rosa P, et al. Storage and release of ATP from astrocytes in culture. J Biol Chem 2003; 278:1354-62; PMID:12414798; http://dx.doi.org/10.1074/jbc.M209454200
36. Bodin P, Burnstock G. Evidence that release of adenosine triphosphate from endothelial cells during increased shear stress is vesicular. J Cardiovasc Pharmacol 2001; 38:900-8; PMID:11707694; http://dx.doi.org/10.1097/00005344-200112000-00012
37. Pangrsic T, Potokar M, Stenovec M, Kreft M, Fabbretti E, Nistri A, et al. Exocytotic release of ATP from cultured astrocytes. J Biol Chem 2007; 282:28749-58; PMID:17627942; http://dx.doi.org/10.1074/jbc.M700290200
38. Martins RM, Alves RM, Macedo S, Yoshida N. Starvation and rapamycin differentially regulate host cell lysosome exocytosis and invasion by Trypanosoma cruzi metacyclic forms. Cell Microbiol 2011; 13:943-54; PMID:21501360; http://dx.doi.org/10.1111/j.1462-5822.2011.01590.x
39. Steffen A, Le Dez G, Poincloux R, Recchi C, Nassoy P, Rottner K, et al. MT1-MMP-dependent invasion is regulated by TI-VAMP/VAMP7. Curr Biol 2008; 18:926-31; PMID:18571410; http://dx.doi.org/10.1016/j.cub.2008.05.044
40. Mili S, Moissoglu K, Macara IG. Genome-wide screen reveals APC-associated RNAs enriched in cell protrusions. Nature 2008; 453:115-9; PMID:18451862; http://dx.doi.org/10.1038/nature06888
41. Tuloup-Minguez V, Greffard A, Codogno P, Botti J. Regulation of autophagy by extracellular matrix glycoproteins in HeLa cells. Autophagy 2011; 7:27-39; PMID:20980830; http://dx.doi.org/10.4161/auto.7.1.13851
42. Martinez-Arca S, Arold S, Rudge R, Laroche F, Galli T. A mutant impaired in SNARE complex dissociation identifies the plasma membrane as first target of synaptobrevin 2. Traffic 2004; 5:371-82; PMID:15086786; http://dx.doi.org/10.1111/j.1398-9219.2004.00180.x
43. Korolchuk VI, Saiki S, Lichtenberg M, Siddiqi FH, Roberts EA, Imarisio S, et al. Lysosomal positioning coordinates cellular nutrient responses. Nat Cell Biol 2011; 13:453-60; PMID:21394080; http://dx.doi.org/10.1038/ncb2204
44. Cantalupo G, Alifano P, Roberti V, Bruni CB, Bucci C. Rab-interacting lysosomal protein (RILP): the Rab7 effector required for transport to lysosomes. EMBO J 2001; 20:683-93; PMID:11179213; http://dx.doi.org/10.1093/emboj/20.4.683
45. Wang T, Ming Z, Xiaochun W, Hong W. Rab7: role of its protein interaction cascades in endo-lysosomal traffic. Cell Signal 2011; 23:516-21; PMID:20851765; http://dx.doi.org/10.1016/j.cellsig.2010.09.012
46. Harrison RE, Bucci C, Vieira OV, Schroer TA, Grinstein S. Phagosomes fuse with late endosomes and/or lysosomes by extension of membrane protrusions along microtubules: role of Rab7 and RILP. Mol Cell Biol 2003; 23:6494-506; PMID:12944476; http://dx.doi.org/10.1128/MCB.23.18.6494-6506.2003
47. Jordens I, Fernandez-Borja M, Marsman M, Dusseljee S, Janssen L, Calafat J, et al. The Rab7 effector protein RILP controls lysosomal transport by inducing the recruitment of dynein-dynactin motors. Curr Biol 2001; 11:1680-5; PMID:11696325; http://dx.doi.org/10.1016/S0960-9822(01)00531-0
48. Santama N, Krijnse-Locker J, Griffiths G, Noda Y, Hirokawa N, Dotti CG. KIF2beta, a new kinesin superfamily protein in non-neuronal cells, is associated with lysosomes and may be implicated in their centrifugal translocation. EMBO J 1998; 17:5855-67; PMID:9774330; http://dx.doi.org/10.1093/emboj/17.20.5855
49. Matsushita M, Tanaka S, Nakamura N, Inoue H, Kanazawa H. A novel kinesin-like protein, KIF1Bbeta3 is involved in the movement of lysosomes to the cell periphery in non-neuronal cells. Traffic 2004; 5:140-51; PMID:15086790; http://dx.doi.org/10.1111/j.1600-0854.2003.00165.x
50. Pankiv S, Alemu EA, Brech A, Bruun JA, Lamark T, Overvatn A, et al. FYCO1 is a Rab7 effector that binds to LC3 and PI3P to mediate microtubule plus end-directed vesicle transport. J Cell Biol 2010; 188:253-69; PMID:20100911; http://dx.doi.org/10.1083/jcb.200907015
51. Cardoso CM, Groth-Pedersen L, Høyer-Hansen M, Kirkegaard T, Corcelle E, Andersen JS, et al. Depletion of kinesin 5B affects lysosomal distribution and stability and induces peri-nuclear accumulation of autophagosomes in cancer cells. PLoS One 2009; 4:e4424; PMID:19242560; http://dx.doi.org/10.1371/journal.pone.0004424
52. Ravikumar B, Moreau K, Jahreiss L, Puri C, Rubinsztein DC. Plasma membrane contributes to the formation of pre-autophagosomal structures. Nat Cell Biol 2010; 12:747-57; PMID:20639872; http://dx.doi.org/10.1038/ncb2078
53. Bal-Price A, Moneer Z, Brown GC. Nitric oxide induces rapid, calcium-dependent release of vesicular glutamate and ATP from cultured rat astrocytes. Glia 2002; 40:312-23; PMID:12420311; http://dx.doi.org/10.1002/glia.10124
54. Di Virgilio F. Liaisons dangereuses: P2X(7) and the inflammasome. Trends Pharmacol Sci 2007; 28:465-72; PMID:17692395; http://dx.doi.org/10.1016/j.tips.2007.07.002
55. Ghiringhelli F, Apetoh L, Tesniere A, Aymeric L, Ma Y, Ortiz C, et al. Activation of the NLRP3 inflammasome in dendritic cells induces IL-1beta-dependent adaptive immunity against tumors. Nat Med 2009; 15:1170-8; PMID:19767732; http://dx.doi.org/10.1038/nm.2028
56. Aymeric L, Apetoh L, Ghiringhelli F, Tesniere A, Martins I, Kroemer G, et al. Tumor cell death and ATP release prime dendritic cells and efficient anticancer immunity. Cancer Res 2010; 70:855-8; PMID:20086177; http://dx.doi.org/10.1158/0008-5472.CAN-09-3566
57. Kreda SM, Okada SF, van Heusden CA, O'Neal W, Gabriel S, Abdullah L, et al. Coordinated release of nucleotides and mucin from human airway epithelial Calu-3 cells. J Physiol 2007; 584:245-59; PMID:17656429; http://dx.doi.org/10.1113/jphysiol.2007.139840
58. Rieg T, Vallon V. ATP and adenosine in the local regulation of water transport and homeostasis by the kidney. Am J Physiol Regul Integr Comp Physiol 2009; 296:R419-27; PMID:19020292; http://dx.doi.org/10.1152/ajpregu.90784.2008
59. Hovater MB, Olteanu D, Welty EA, Schwiebert EM. Purinergic signaling in the lumen of a normal nephron and in remodeled PKD encapsulated cysts. Purinergic Signal 2008; 4:109-24; PMID:18438719; http://dx.doi.org/10.1007/s11302-008-9102-6
60. Lee JH, Marcus DC. Purinergic signaling in the inner ear. Hear Res 2008; 235:1-7; PMID:17980525; http://dx.doi.org/10.1016/j.heares.2007.09.006
61. Oury C, Toth-Zsamboki E, Vermylen J, Hoylaerts MF. The platelet ATP and ADP receptors. Curr Pharm Des 2006; 12:859-75; PMID:16515502; http://dx.doi.org/10.2174/138161206776056029
62. Martins I, Tesniere A, Kepp O, Michaud M, Schlemmer F, Senovilla L, et al. Chemotherapy induces ATP release from tumor cells. Cell Cycle 2009; 8:3723-8; PMID:19855167; http://dx.doi.org/10.4161/cc.8.22.10026
63. Michaud M, Martins I, Sukkurwala AQ, Adjemian S, Ma Y, Pellegatti P, et al. Autophagy-dependent anticancer immune responses induced by chemotherapeutic agents in mice. Science 2011; 334:1573-7; PMID:22174255; http://dx.doi.org/10.1126/science.1208347
64. Martinez-Arca S, Alberts P, Galli T. Clostridial neurotoxin-insensitive vesicular SNAREs in exocytosis and endocytosis. Biol Cell 2000; 92:449-53; PMID:11132707; http://dx.doi.org/10.1016/S0248-4900(00)01096-0
65. Edelstein A, Amodaj N, Hoover K, Vale R, Stuurman N. Computer control of microscopes using microManager. Curr Protoc Mol Biol 2010; Chapter 14:Unit14